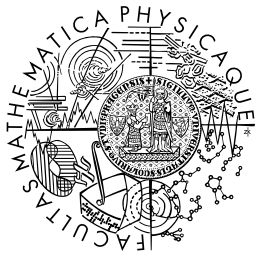

FACULTY
OF MATHEMATICS
AND PHYSICS
Charles University

DOCTORAL THESIS

Václav Pavlík

Perturbed Stellar Motion in Dense Star Clusters

Astronomical Institute of Charles University

Adviser of the thesis:	doc. RNDr. Ladislav Šubr, Ph.D.
Study programme:	Theoretical Physics, Astronomy and Astrophysics

Prague 2019

Prohlašuji, že jsem tuto dizertační práci vypracoval samostatně a výhradně s použitím citovaných pramenů, literatury a dalších odborných zdrojů.

Beru na vědomí, že se na moji práci vztahují práva a povinnosti vyplývající ze zákona č. 121/2000 Sb., autorského zákona v platném znění, zejména skutečnost, že Univerzita Karlova má právo na uzavření licenční smlouvy o užití této práce jako školního díla podle §60 odst. 1 autorského zákona.

I declare that I carried out this doctoral thesis independently, and only with the cited sources, literature and other professional sources.

I understand that my work relates to the rights and obligations under the Act No. 121/2000 Coll., the Copyright Act, as amended, in particular the fact that the Charles University has the right to conclude a license agreement on the use of this thesis as a school work pursuant to Section 60 paragraph 1 of the Copyright Act.

In Prague, 25th June 2019 .....

Title:
Perturbed Stellar Motion in Dense Star Clusters

Author:
RNDr. Václav Pavlík
( https://orcid.org/0000-0002-3031-062X)

Department:
Astronomical Institute of Charles University

Adviser:
doc. RNDr. Ladislav Šubr, Ph.D.
(Astronomical Institute of Charles University)

Keywords:
– methods: numerical, analytical, data analysis
– techniques: N-body simulations
– star clusters: general, individual: Orion Nebula Cluster
– stars: formation, evolution, binaries, neutron stars, black holes
– Galaxy: general

Abstract:
Star clusters are thought to be the birthplaces of stars as well as the building blocks of galaxies. They typically consist of thousands to millions of stars bound together by self-gravity. These systems evolve on the scale of Myr to Gyr, therefore, it is impossible for us to see any change in their global evolution even within hundreds of human lifetimes.

Although the equations of motion of stars in a star cluster are simple Newtonian, it is impossible to predict precisely history of any star within them to any point in the future. Therefore, we may either compare the observations of different star clusters at different age, we may invent theoretical approaches and analytical predictions, or we must follow their evolution numerically (e.g. with direct N-body integrators) which is the main focus of my research and this thesis.

First, we follow the evolution of star clusters in general while coming up with a novel method to estimate their characteristic timescale (i.e. the time of core collapse) based on global parameters. The core collapse is directly linked to the formation of hard binary stars, thus, we focus on their analysis as well. We also follow several recent observational results:

(i) *ALMA* observations of the Serpens South star-forming region indicate that star clusters are born mass segregated. But in the evolved clusters, this primordial mass segregation seems to be lost. We are the first to present an empirical estimate based on numerical simulations of the timescale on which the primordial mass segregation vanishes. We also apply our results on the Orion Nebula Cluster (for that we compiled the most complete dataset of this cluster yet, which is now also available online).

(ii) Galactic globular clusters are observed to contain up to 50 % of black holes. In order to constrain the initial retention fraction of black holes within them, we made a series of numerical models and an analytic model.

(iii) Finally, we looked at star clusters from a more global view in the Galaxy. We found that the recently measured γ-ray excess from the centre of our Galaxy may be due to millisecond pulsars which were deposited there by inspiraling and tidally disrupted globular clusters.

Název práce:
Perturbed Stellar Motion in Dense Star Clusters

Autor:
RNDr. Václav Pavlík
(https://orcid.org/0000-0002-3031-062X)

Katedra:
Astronomický ústav Univerzity Karlovy

Vedoucí:
doc. RNDr. Ladislav Šubr, Ph.D.
(Astronomický ústav Univerzity Karlovy)

Klíčová slova:
– metody: numerické, analytické, datová analýza
– techniky: N-částicové simulace
– hvězdokupy: obecné, individuální: Velká mlhovina v Orionu
– hvězdy: vznik, vývoj, dvojhvězdy, neutronové hvězdy, černé díry
– Galaxie: obecné

Abstrakt:
Hvězdokupy jsou považovány za místa, kde se rodí hvězdy, a za stavební kameny galaxií. Skládají se obvykle z tisíců až milionů hvězd, které jsou pospolu držené svou vlastní gravitací. Tyto soustavy hvězd se vyvíjejí na škálách milionů až miliard roků, takže je nemožné pozorovat jejich celkový vývoj přímo ani po stovky lidských generací.

Navzdory tomu, že chování hvězd uvnitř hvězdokup lze popsat jen Newtonovými pohybovými rovnicemi, nemůžeme nikdy předpovědět jejich přesné dráhy do budoucnosti. Proto nám nezbývá než porovnávat pozorování hvězdokup v různých stádiích vývoje, vymýšlet teoretické postupy a analytické odhady, nebo použít ke zkoumání hvězdokup numerické metody (např. přímý N-částicový integrátor), což je také hlavním zaměřením mého výzkumu a této práce.

Nejprve jsme se zaměřili na vývoj hvězdokup obecně, přičemž jsme přišli s novou metodou, jak odhadnout jejich charakteristický čas vývoje (tj. čas kolapsu jádra) na základě globálních parametrů. Kolaps jádra je přímo spojen s tvorbou silně vázaných dvojhvězd, takže jsme se věnovali i jejich studiu. Také jsme navázali na několik nedávných výsledků pozorování:

(i) Data z rodící se hvězdokupy v mlhovině Serpens South (v souhvězdí Hada), získaná na observatoři *ALMA*, ukazují, že se hvězdy ve hvězdokupách rodí zcela hmotnostně uspořádané, což ale u vyvinutějších hvězdokup už není tak zřejmě vidět. Byli jsme první, kdo na základě numerických modelů učinil empirický odhad časové škály, na které hvězdokupy o své počáteční hmotnostní uspořádání přijdou. Naše výsledky jsme také aplikovali na Velkou mlhovinu v Orionu (při tom jsme zkompilovali asi dosud nejucelenější databázi zdrojů v této hvězdokupě, která je k dispozici online).

(ii) Kulové hvězdokupy v naší Galaxii obsahují až 50 % ze své původní populace černých děr. Abychom omezili prostor parametrů zodpovědných za počáteční zadržování černých děr v těchto systémech, vypočítali jsme sadu numerických modelů a vytvořili i analytický model.

(iii) Na závěr jsme se též zaměřili na hvězdokupy a jejich vliv na naši Galaxii. Zjistili jsme, že nedávno objevený výkyv γ-záření z centra Galaxie může být způsobený millisekundovými pulzary. Ty byly do jádra Galaxie dopraveny jako součást populace hvězd v kulových hvězdokupách, jež tam domigrovaly a následně byly slapově roztrhány.

"If we lived on a planet where nothing ever changed, there would be little to do. There would be no impetus for science. And if we lived in an unpredictable world, where things changed in random or very complex ways, we would not be able to figure things out. Again, there would be no such thing as science. But we live in an in-between universe, where things change, but according to patterns, rules, or, as we call them, laws of nature. If I throw a stick up in the air, it always falls down. If the sun sets in the west, it always rises again the next morning in the east. And so it becomes possible to figure things out. We can do science, and with it we can improve our lives."

— Carl Sagan, Cosmos

Acknowledgements

First and foremost, I would like thank my family for their support. I would like to also express my gratitude to Steve Shore for his perpetual support, enthusiasm, coffee and 2D N-body practice sessions (otherwise known as billiard), and also for his help, comments and for proof-reading the manuscript while I was finalising this thesis. Further, I would like to thank Douglas Heggie, Pavel Kroupa, Sverre Aarseth and Giacomo Fragione for their selfless guidance and mentorship, and ideas for new research projects. Last but not least, I would like to thank my adviser, Ladislav Šubr, everyone with whom I had the opportunity to work on scientific articles, and also my colleagues for discussions and fun in the office.

I deeply acknowledge support from Charles University, especially from the former and current directors of the Astronomical Institute – Marek Wolf and David Vokrouhlický – who provided a good environment, recognised my scientific work as well as my involvement in popularisation of astronomy and teaching, and offered financial support whenever needed. I am also grateful for the financial support from my own university grant (GAUK-186216), from the grant dedicated to the Specific Scientific Research (SVV-260441) and from the Czech Science Foundation through the project of Excellence No. 14-37086G.

Numerical simulations and data analysis of the scale needed for this work would not be possible to realise without access to the computing and storage facilities owned by parties and projects contributing to the National Grid Infrastructure MetaCentrum, provided under the programme "Projects of Large Research, Development, and Innovations Infrastructures" (CESNET LM2015042), which I greatly appreciate.

Contents

1. Premise

Since the dawn of civilisations, people have looked at the sky in amazement and with sacred respect. They have followed the movement of celestial bodies, related to their deities, on which they based the calendar and their notion of time. They found out that periodically repeating events coincide with certain tasks during a year which were necessary for their survival and well-being. For the Maya, the heliacal rise of the Pleiades (in other cultures the star Spica) was related to a harvest season. When the star Sirius appeared on sky first time in a year, this was an indication for the ancient Egyptians that there will be floods on Nile. Similar examples are documented across many cultures. These observations had an impact not only on astronomy[1] and religion but also on mathematics, as there was the urge to calculate the positions and separation of planets, politics or architecture, as new ways of building were employed to realise the necessity to honour gods with temples and monuments (e.g. the Temple of Hathor in Dendera). Certain areas of the starry sky were also dedicated to commemorate historic or heroic events from various myths and legends, or to honour the deed of the emperor himself. For each culture the stars and constellations were different. For instance, the nights in winter show an epic fight of the hunter Orion with a fierce bull – that is what the Greeks saw and what also propagated into the modern history. For the Maya, the same stars represented the myth of creation of the world. Three stars from our constellation of Orion – Alnitak, Rigel and Saiph – represented three

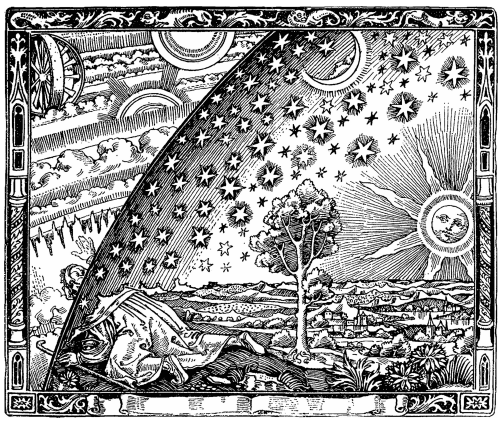

Figure 1.1: A metaphoric depiction of acquiring knowledge through science and experiments. Taken from Nicolas Camille Flammarion, L'Atmosphère: Météorologie Populaire (Paris, 1888).

[1] More precisely *astrology*, but such a term may only be permitted in a footnote.

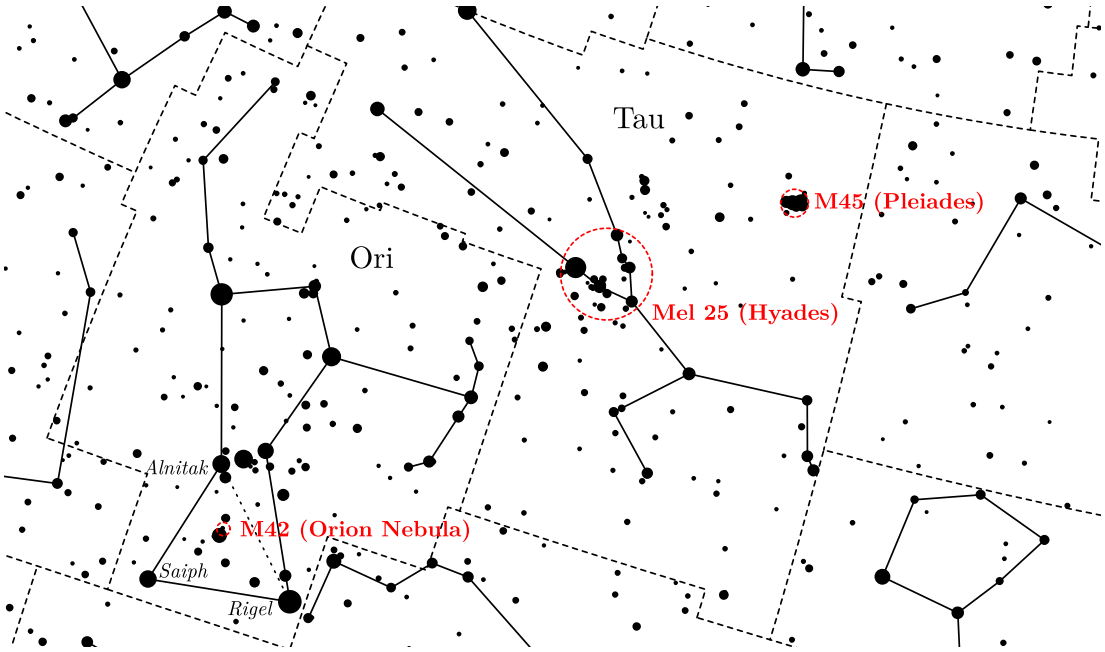

Figure 1.2: The constellations of Orion and Taurus (from SkyMap) with three representatives of open clusters: the Orion Nebula, Pleiades and Hyades, with their designation in the Messier or Melotte catalogue.

stones of a sacred fireplace and the Orion sword with θ Ori in the middle was the rising smoke. It is due to invention and technology that we now see past the myths and perceive the world differently; we can probe it, discover what forms it, and aspire to an understanding of how everything works (see Fig. 1.1). Indeed, we discovered the "universe" as an organising principle to the real world. We were able to deduce that the Earth is neither flat nor on top of a shell of a giant turtle nor the centre of the cosmos. That it is a medium-sized planet orbiting an ordinary G-type dwarf star at a convenient distance for a particular sort of life to evolve on its surface, and together with billions of other stars and planets is part of our Galaxy. Nonetheless, the beauty of the night sky still motivates and inspires us.

For somebody who studies star clusters – objects that are considered to be the birthplaces of stars and the building blocks of galaxies – the northern winter sky offers a unique "time machine". As star clusters typically evolve on a time scale of millions of years, being able to catch at least a glimpse of their global evolution is not possible even within hundreds of human lifetimes. Yet during winter nights in the northern hemisphere, we can see the Orion Nebula Cluster (ONC), the Pleiades and the Hyades high above the southern horizon together at the same time, as illustrated in Fig. 1.2. Those three objects are all very similar and classified as open clusters (in the case of the ONC, an embedded cluster). Their age is roughly 2.5 Myr (Hillenbrand 1997; Palla & Stahler 1999), 100 Myr (Kroupa et al. 2001) and about 680 Myr (Cummings & Kalirai 2018), respectively. Although we will remain unable to visually observe the ONC for another 100 Myr, we can grasp what is probably going to happen to it by looking at the Pleiades (Kroupa et al. 2001) etc.

2. Introduction

Star clusters typically consist of thousands to millions of stars bound together by the same gravitational force that keeps the Moon in orbit and causes apples to fall from trees in a garden in Lincolnshire. Being composed of so many bodies, star clusters are very complex in a dynamical sense. Thus, it is impossible to precisely know the dynamical history of any single star within them or to predict it to any point in the future, despite being able to write the equations of motion of each component. Gravity is the dominant force in star clusters. Thus, we do not even need complicated theories and these equations may be the simplest ones imaginable – the Newtonian equations of motion. The acceleration of the i-th star is given by the superposition of the gravitational pull from all the other stars

$$\ddot{\boldsymbol{r}}_i = -G \sum_{j=1,\, j\neq i}^{N} m_j \frac{\boldsymbol{r}_i - \boldsymbol{r}_j}{|\boldsymbol{r}_i - \boldsymbol{r}_j|^3}\,, \tag{2.1}$$

where $\boldsymbol{r}$ is the position vector and m is the mass of a particular body, G is the gravitational constant, N is the total number of stars in the system and dot represents the derivative with respect to time. As these are $3N$ second order ordinary differential equations, we have to prescribe $6N$ initial conditions in order to solve them. In practice, we use three Cartesian coordinates and three velocity components for each star, and in more complicated systems, we also assign a non-unity mass to each star. We already face many decisions and free parameters to choose, yet we are just setting up the initial conditions.

Newtonian gravitation is a good approximation for a lot of systems in the weak field limit if we neglect gas dynamics and are not concerned with relativistic effects – e.g. black hole (BH) or neutron star (NS) coalescence, or the emission of gravitational waves. In the N-body problem, we further assume that stars are point masses. This is, again, a simplification but it works reasonably well if the separation of two stars is substantially greater than the sum of their radii and if the mergers of stars or tidal effects are unimportant.

An obvious problem with the equations of motion (2.1) is that the denominator goes to zero and the whole sum explodes to infinity if two stars approach very closely or collide (assuming point masses, collisions should not happen since the model stars have no real dimension but in practice, floating point precision is finite and enables two stars to be at the same time at the same coordinates). We can overcome this problem by introducing a parameter of constant minimum distance, ε, in the denominator of the force law (Aarseth 2003), such that

$$|\boldsymbol{r}_i - \boldsymbol{r}_j|^3 \;\rightarrow\; \left(|\boldsymbol{r}_i - \boldsymbol{r}_j|^2 + \varepsilon^2\right)^{3/2}\,.$$

For large separations, the effect of ε is negligible. But if two bodies closely approach each other, it dominates. It "softens" the force and prevents the sum from going to infinity, although at the cost of a physically imprecise result. This approach is, therefore, not practicable in systems where close encounters play a role, such as star clusters, where binary stars are an important element. It may be, however, applied in small-N models where high precision is not essential. Modification of the gravitational force at short distances was first introduced by Bošković (1763, English translation of the Latin manuscript is from 1922), see also Fig. 2.1. The argument that gravity does not work the same way on very small scales[1] was based on the observational evidence, e.g., that gas particles use to repulse each other and the whole volume rather expands instead of collapsing gravitationally. Although this reasoning was not entirely correct, he was the first to point out the singularity in Eq. (2.1) and proposed a way to deal with it. Nowadays, we may see an analogy in the thermodynamic approach of van der Waals despite it being formally different – gas molecules are surrounded by a fixed finite volume (to give more realistic interactions than provided in an ideal gas). In the N-body framework, the idea of a softening parameter arose again from the discussion of S. J. Aarseth and F. Hoyle (private communication with S. J. Aarseth, March 2019) and was first introduced in the N-body calculations of galaxy clusters where ε represents the effective size of a galaxy (Aarseth 1963). We may see an analogy with this also in the softened star cluster's potential – first derived by Schuster (1883) for the interior of the Sun, later given another astrophysical meaning as the best fit for the observed star cluster profiles (Plummer 1911). Now it is often used for the initial conditions of star clusters due to its simple analytical form

$$\Phi(r) = -\frac{GM}{\sqrt{r^2 + r_{\mathrm{P}}^2}}\,, \tag{2.2}$$

where M is the system's total mass and r_{P} is the scale (Plummer) radius, i.e. softening. And in late-70s, a sort of softening was adopted as the basis for smoothed-

Figure 2.1: Croatian 100 dinar note with the portrait of J. R. Bošković and three figures from his treatise on gravitation.

[1] As summarised in the side-note of Art. 121: *"Non obesse theoriam gravitatis; cujus lex in minimis distantiis locum non habet."*, meaning that although we do not oppose the theory of gravitation, it does not work for very small distances.

particle hydrodynamics, with each smoothed-particle occupying a finite volume in space (Lucy 1977; Monaghan & Gingold 1977).

The complexity of an N-body problem in its purest form, i.e. using Eq. (2.1), is $O(N^2)$. Therefore, we often use computers running dedicated codes with algorithms for solving the equations of motion as efficiently and precisely as possible. Specialised hardware has also been developed to increase the efficiency and to lower the computational time (and therefore the cost of calculations). For instance, the GRAPE[2] GPU was specially designed to rapidly calculate the gravitational interaction between two particles (the first version, GRAPE-1, was introduced by Ito et al. 1990). Since then, extensive upgrades have been made, now there are generations GRAPE-6 and GRAPE-DR[3] (Yuen et al. 2013) and also possibilities to mimic GRAPE-6 on other GPUs (Gaburov et al. 2009). With a large number of stars in a cluster model (i.e. approaching realistic star cluster size of hundreds of millions), direct summation would still be too slow and expensive even with a dedicated high-end hardware. Optimisation of the force calculation is, therefore, still necessary.

One of the minor optimisations is in choosing the right set of units for the problem we investigate and the model we want to calculate. This approach may reduce the number of floating point operations to the absolute minimum, yielding higher precision and somewhat quicker calculation. Setting the gravitational constant, G, to unity is an obvious first step. If the object of interest is the Solar system (or even an isolated few-body interaction), it is convenient to express time in years, distance in astronomical units and velocity in the multiples of $30\,\mathrm{km\,s^{-1}}$ (the approximate Earth's orbital speed). For N-body modelling of star clusters, the commonly used units are so called "Hénon units" (Heggie 2014), i.e. $G = M = -4E = 1$, where E stands for the total energy of the system (negative sign means a bound system). In those units, a scale radius of the system (i.e. virial radius; see Sect. 3.2) is also equal to one.

To reduce the $O(N^2)$ dependence of N-body calculations to a more manageable level, many different techniques of numerical modelling have been employed. A community-wide standard code for a single CPU, `nbody6`, and its implementation for parallel computing on CPUs (with SSE[4]) and GPU (Aarseth 2003; Nitadori & Aarseth 2012) is specifically designed to study collisional stellar dynamical systems and incorporates many of these techniques. It is a *direct N-body code* using a fourth order Hermite predictor–corrector integration scheme (Makino 1991) with individual time-steps. Gravitational interaction between distant stars may be evaluated less frequently than in the case of near stars, thus it is divided into regular and irregular force based on the Ahmad–Cohen neighbour scheme (Ahmad & Cohen 1973; Makino & Aarseth 1992). Close encounters of stars, where Eq. (2.1) is singular, can be specially treated without the need of softening in another and more suitable coordinate system – i.e. a regularisation (Kustaanheimo & Stiefel 1965; Aarseth & Zare 1974; Mikkola & Aarseth 1990, 1993). A combination of these methods is used to achieve the highest performance possible.

[2]GRAvity PipE

[3]Greatly Reduced Array of Processor Elements with Data Reduction

[4]Streaming SIMD (Single Instruction Multiple Data) Extensions

While exploring star cluster evolution numerically, we are not limited to direct summation N-body codes to solve Eq. (2.1). Several other approaches exist. To predict the general evolution of a star cluster (e.g. the core collapse), the whole system can be treated as an ideal gas. Such a model will then obey the equations of fluid dynamics. However, star clusters are different from the ideal gas, e.g. the mean free path of a particle (star) in a cluster is much longer than in a gas model (Spitzer 1987), so the results obtained using gaseous models may have to be verified by different and more accurate techniques. Other methods rely, e.g., on solving the Fokker–Planck equation, which is a Boltzmann equation with an encounter term on the right-hand side expressed via the diffusion coefficients up to the first order

$$\frac{\mathrm{d}f(\boldsymbol{r},\boldsymbol{v},t)}{\mathrm{d}t} = \left(\frac{\partial f}{\partial t}\right)_{\mathrm{enc}},$$

$$\text{with } \left(\frac{\partial f}{\partial t}\right)_{\mathrm{enc}} = -\sum_{i=1}^{3}\frac{\partial(f\langle\Delta v_i\rangle)}{\partial v_i} + \frac{1}{2}\sum_{j=1}^{3}\frac{\partial^2(f\langle\Delta v_i\Delta v_j\rangle)}{\partial v_i \partial v_j}\,. \tag{2.3}$$

Here f is the velocity distribution function which depends on the position vector $\boldsymbol{r}$, the velocity vector $\boldsymbol{v}$ and time t, $\langle\Delta v_i\rangle$ represent the coordinates of the diffusion coefficient and $\langle\Delta v_i\Delta v_j\rangle$ are the coordinates of the tensor coefficient. These coefficients come from the sum of changes $\Delta\boldsymbol{v}$ and $\Delta\boldsymbol{v}\Delta\boldsymbol{v}$ over all encounters, respectively. Eq. (2.3) thus describes quantitatively the diffusion in velocity space as a result of cumulative velocity changes, where these changes have to be smaller than the actual velocity (e.g. Cohen et al. 1950; Spitzer 1987). This approach enables us to calculate larger systems than those possible with direct N-body methods. However, for $\Delta v \approx v$ (e.g. when binary stars start to form or when the system goes through core collapse), Eq. (2.3) becomes invalid. Hybrid codes that treat binaries near the core as a separate N-body problem from the rest of the cluster may be used here to evolve the star cluster through and beyond the core collapse (e.g. McMillan & Lightman 1984). This approach is quicker than direct N-body integrators which is an important advantage but on the other hand, it is, e.g., unable to provide information about the rate of escaping stars.

Independently, Eq. (2.3) may be solved also using one of the family of Monte Carlo (MC) methods. Although they are less precise than the direct solution of the Fokker–Planck equation, they offer other advantages. Two basic methods are distinguished – the Hénon method (or orbit-averaged MC method; Hénon 1971a,b; Hénon 1973) and the Princeton method (or dynamical MC method; Spitzer & Thuan 1972). Stars are not treated individually but rather as ensembles with the same properties (e.g. in spherical shells). We are not following individual trajectories but we are applying velocity perturbation to these groups according to known probabilities. Precise algorithms and means of computing depend on the method used whose discussion is not the intent of this thesis. Therefore, we will not go in further details.

None of the approaches mentioned above is exact, nor can any represent precisely real objects. We may, however, reliably use them to *statistically* evaluate different evolutionary aspects or properties of these systems. The application of direct N-body simulations to star clusters is the main focus of this thesis and the attached papers. The work is structured as follows: first, we focus on the

formation and evolution of star clusters, then we discuss the effect of sub-systems of the cluster (e.g. binary stars, neutron stars, black holes) on their evolution and vice versa, and finally we discuss the behaviour of a star cluster in the Galaxy. To conclude, we present ideas for future research, discussion of several key issues and the implications for future research that arise from this work. All the methods used and detailed results are presented in the attached papers; key results are given in the main text of the thesis.

3. Star cluster formation and evolution

The evolution of a star cluster occurs on two timescales – relaxation and crossing times. The relaxation time, which is a characteristic time for global evolution, is caused by two-body encounters and derived by evaluating the behaviour of a pair of stars after a close approach and averaging the resulting effect over the whole cluster. In an environment with a greater concentration of stars (e.g. the cluster core), individual stellar encounters are more frequent so the relaxation time is shorter. Similarly, with an increasing velocity dispersion, two-body interactions are less important and the relaxation time increases. The relaxation time depends strongly on the radial distance from the cluster centre. Thus, for a global measure of the process, we use the median relaxation time ($t_{\rm rh}$; Spitzer & Hart 1971a) where the velocity dispersion is replaced by the mean-square speed and the density is associated with the half-mass radius ($r_{\rm h}$; a radius of a sphere around the centre of the cluster containing half of the total mass of the cluster, M). This gives a relation based on global parameters

$$t_{\rm rh} \approx \frac{0.138N}{\ln\left(0.4N\right)}\sqrt{\frac{r_{\rm h}^3}{GM}}\,, \tag{3.1}$$

where N is the total number of stars and G is the Newtonian gravitational constant (e.g. $G \approx 4.49 \times 10^{-3}\,{\rm pc}^3 M_\odot^{-1}{\rm Myr}^{-2}$).

The crossing time, $t_{\rm cr}$, is a scale for local changes given, e.g., by few-body encounters. As the name suggests, it is equal to the time needed for a star of a typical speed (e.g. the mean-square speed) to traverse the cluster unperturbed (Binney & Tremaine 1994),

$$t_{\rm cr} = \frac{R}{v_{\rm typ}}\,. \tag{3.2}$$

Assuming a state of approximate equilibrium, the crossing time comes from the global parameters as well (cf. Aarseth 2003)

$$t_{\rm cr} \approx 2\sqrt{2}\sqrt{\frac{2.2r_{\rm h}^3}{GM}}\,. \tag{3.3}$$

When expressed in Hénon units, the second square root is equal to 1, leaving $t_{\rm cr} = 2\sqrt{2}$.

3.1 Mass segregation

Any star moving in a field of stars act on its surroundings gravitationally and feels the gravitational pull of the other stars. It attracts closer stars more than the stars which are away. It also has a greater pull on the stars near its current location than on those which are in its direction of movement. The neighbouring stars are deflected to form a gravitating wake that trails the moving star. Analogous to a fluid, such a star then behaves as if it were passing through a viscous environment which slows it down. We note that it is a local effect in an otherwise collisionless medium and that the whole wake is merely an overdensity resulting from the continuity equation. Being caused by dynamical effects, this phenomenon is called *dynamical friction* (Chandrasekhar & von Neumann 1942, 1943; Chandrasekhar 1943) and the resulting force always opposes the star's motion but unlike fluid viscous drag, it is dissipationless. In a system with an isotropic distribution of velocities $f(v)$, the deceleration of a star of mass m is given by

$$\frac{\mathrm{d}\boldsymbol{v}}{\mathrm{d}t} = -16\pi^2 \ln\Lambda \, G^2 \, m'(m+m') \int_0^v f(v') v'^2 \mathrm{d}v' \, \frac{\boldsymbol{v}}{v^3} \,, \tag{3.4}$$

where v is the star's velocity, m' is the mass of a typical field star and

$$\ln\Lambda \equiv \ln \frac{b_{\max} \, v_{\mathrm{typ}}^2}{G(m+m')} \tag{3.5}$$

is the Coulomb logarithm (named analogously to a logarithm which appears in plasma physics), where $b_{\max}$ is the maximum impact parameter of the pair of encountering stars. The Coulomb logarithm is usually, as in Eq. (3.1), given the value $\ln\Lambda \approx \ln 0.4N$ (e.g. Binney & Tremaine 1994). Being proportional to the mass of the moving star, this force of dynamical friction is stronger for more massive objects. Consequently, it leads to the phenomenon of mass segregation in the cluster: more massive stars tend to be concentrated in the core while less massive ones populate the halo. For slowly moving stars, the integral simplifies and the dynamical friction has only a linear dependence on $\boldsymbol{v}$. For high-velocity stars it remains dependent on the inverse square of the star's velocity. Even a system in which all stars have equal masses experiences dynamical friction, although its effect is weakened.

Mass segregation is, however, not only present in evolved star clusters as a consequence of their dynamical evolution. Recent *ALMA*[1] observations of the Serpens South star-forming region by Plunkett et al. (2018) suggest that newborn clusters are formed completely mass segregated, i.e. the most massive stars are forming in the core while the least massive stars are forming towards the outskirts of the cluster. Independent research by Kirk & Myers (2011) has also documented that very young embedded clusters are mass segregated. As shown by Adams & Fatuzzo (1996) and Matzner & McKee (2000), protostars may control and eventually suppress their accretion through an accretion-induced luminosity. If star formation is self-regulated in such a way, an embedded cluster would be primordially more mass segregated than if the star formation is not self-regulated.

[1] Atacama Large Millimeter/sub-millimeter Array

Understanding this primordial mass segregation is, therefore, important to improve our knowledge of star and star cluster formation.

Methods for creating mass-segregated initial conditions (Baumgardt et al. 2008; Šubr et al. 2008) sort the cluster members in decreasing order of mass and binding energy from the centre of the cluster outwards. The former strictly, the latter statistically. In a collisionless system, the degree of mass segregation could only increase. Thus, if a collisionless system is completely mass segregated primordially, that state persists. Despite observing a general tendency to evolve towards a higher mass segregation even in collisional systems, their degree of mass segregation may both increase and decrease due to two-body encounters that lead to energy equipartition. Consequently, in an evolved star cluster, we may no longer see evidence for its primordial mass segregation after a certain period of time. This motivated our study of how quickly the primordial mass segregation is lost (Pavlík et al. 2019). We integrated an ensemble of N-body models with the Kroupa (2001) initial mass function (IMF), with various total masses and numbers of stars, and for each cluster, we used two extreme primordial mass segregations according to a model of Baumgardt et al. (2008) – either none or complete mass segregation[2]. Our numerical results show that clusters which are primordially fully mass segregated lose that initial property gradually before settling at some level of mass segregation (i.e. they do not lose it completely). Clusters without initial mass segregation establish it dynamically and settle almost at the same level as the primordially segregated do. We have found the time when the difference of mass segregation between both extreme clusters stabilises or even vanishes (denoted as $\tau_{\rm v}$). This was done using spatial integrals under the radial distributions of mean mass in both primordially segregated and non-segregated clusters, $A_{\rm seg}$ and $A_{\rm non}$, respectively, where

$$A = \sum_{k=1}^{n_{\rm bin}} \frac{\langle m(r_k)\rangle}{\Delta r_k}\,. \tag{3.6}$$

Here $\langle m(r_k)\rangle$ is the mean stellar mass up to a radius r_k and Δr_k is the bin width in a logarithmic scale, as plotted in Fig. 3.1 (cf. equations (3) and (4) in Pavlík et al. 2019). For the bin-weighting discussion, see also Appendix C therein.

The time when the primordial difference vanishes is determined from the ratio $A_{\rm seg}/A_{\rm non}$ as the instant when it reaches a constant value, as shown in Fig. 3.2. An empirical estimate of this time is

$$3\,t_{\rm rh} < \tau_{\rm v} < 3.5\,t_{\rm rh}\,. \tag{3.7}$$

This time $\tau_{\rm v}$ seems to be universal, with the mean value in all models around $\langle\tau_{\rm v}\rangle \approx 3.3\,t_{\rm rh}$, which is also plotted for reference in Fig. 3.2. In an ideal case, the ratio $A_{\rm seg}/A_{\rm non} \to 1$ for the different primordial conditions to vanish. We have studied clusters containing from 1.2k to 9.2k stars. In the larger clusters with 4.7k or 9.2k stars, this ratio oscillates around unity; however, in the lower-mass clusters, it stabilises at a slightly higher value between 1 and 2. This is mainly due to early two-body encounters that have greater effect in smaller systems. Moreover, if a system is primordially mass segregated, these early few-body

[2]Complete mass segregation does not imply energy equipartition.

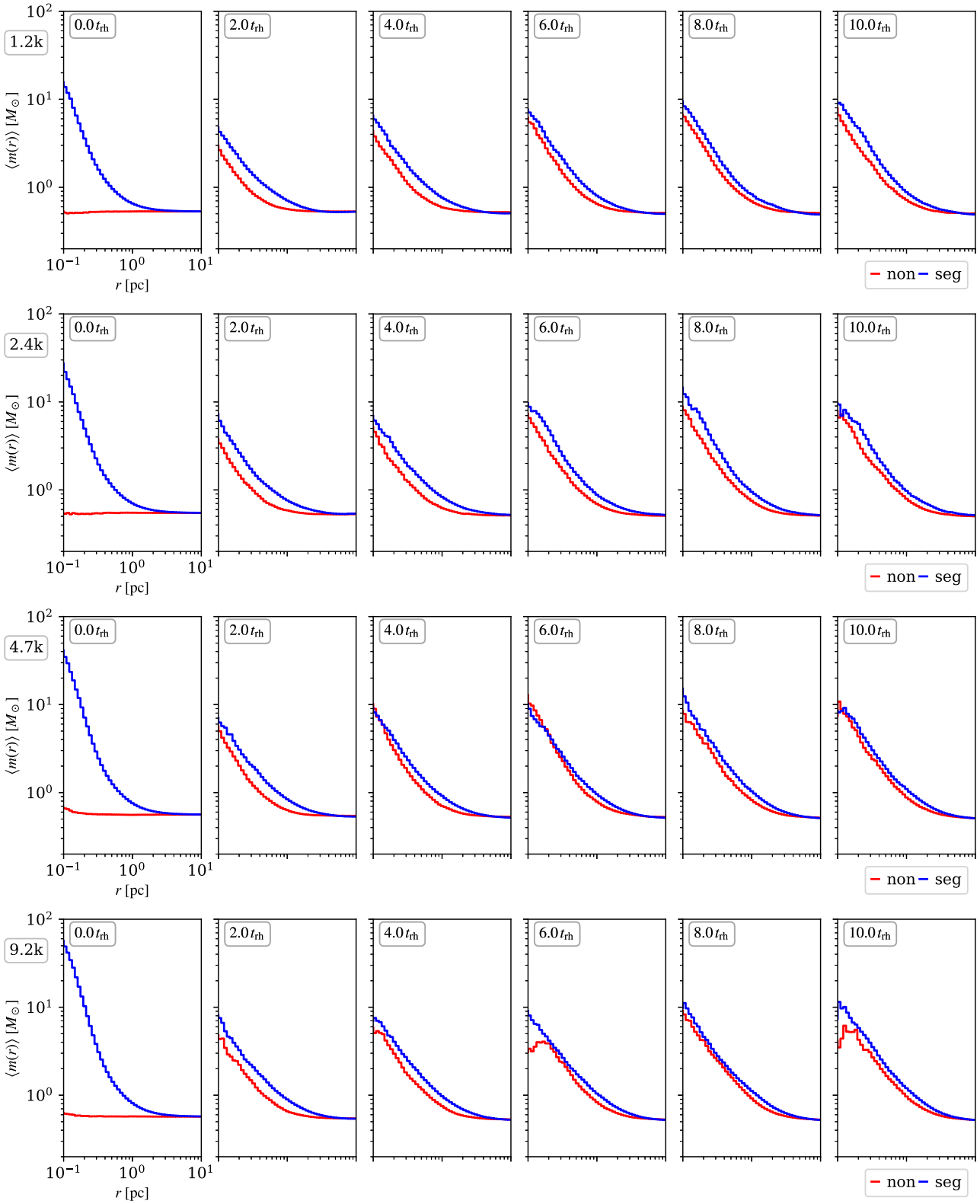

Figure 3.1: The mean mass comprised in a sphere of a given radius of the models with 1.2k, 2.4k, 4.7k and 9.2k stars (from top to bottom). The initially mass segregated models are blue, and the non-segregated are red. (taken from Pavlík et al. 2019)

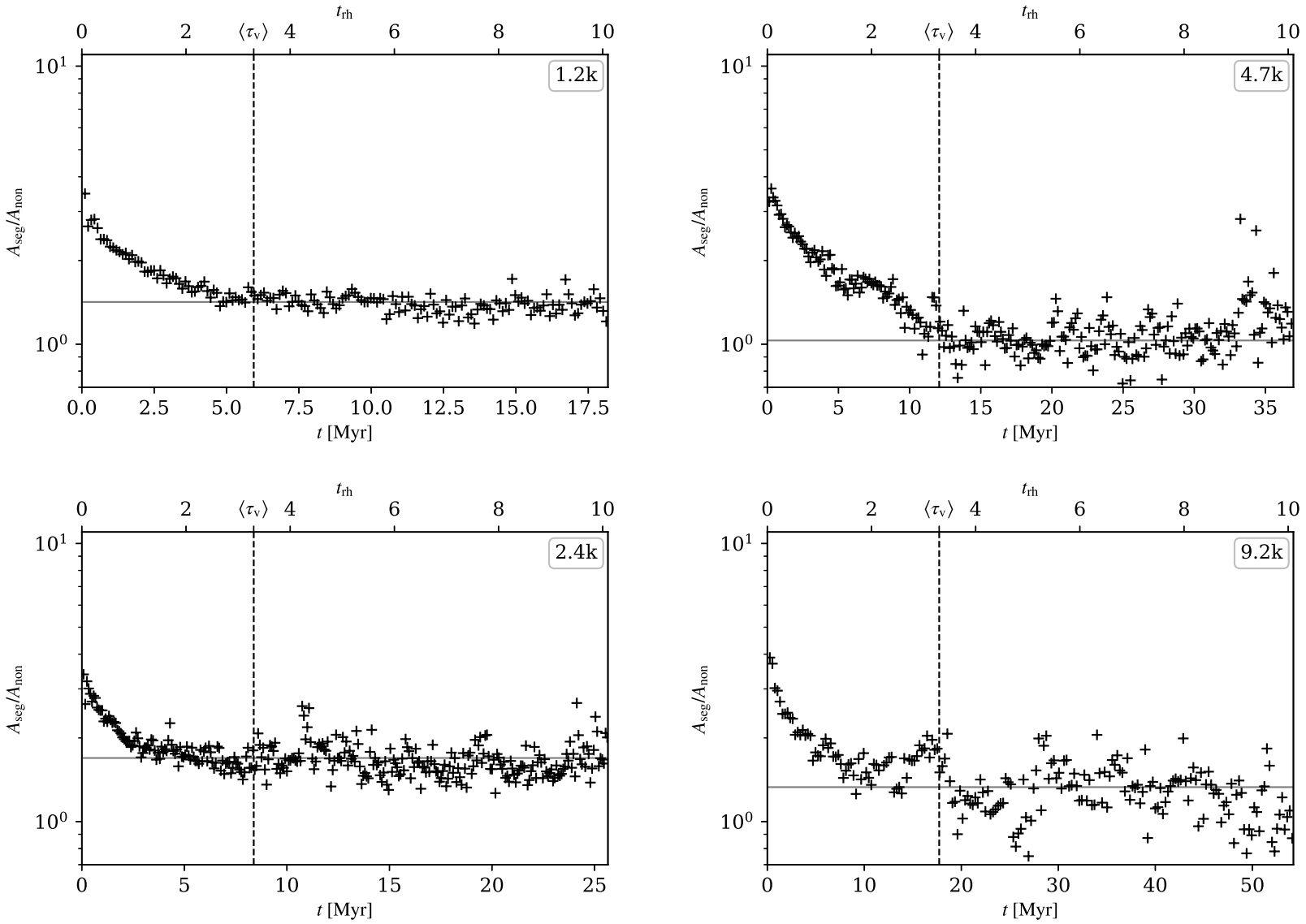

Figure 3.2: The ratio of parameters A under the curves of radial distribution of the mean mass, see Eq. (3.6), of the primordially fully mass segregated and not mass segregated models (see Fig. 3.1). The estimated time τ_v, see Eq. (3.7), when the slope of the data points turned zero is marked by a dashed line. The slope itself is plotted by a grey line. (taken from Pavlík et al. 2019)

interactions will happen more frequently and will be localised near the core, while in the case of a non-segregated cluster, they will occur throughout the cluster and their effect will be weakened. Consequently, a primordially mass segregated cluster will initially inflate more than the non-segregated one (Pavlík et al. 2019), causing the ratio $A_{\rm seg}/A_{\rm non}$ to have a constant non-unity value after $\tau_{\rm v}$ (see the difference between the red and blue curves in Fig. 3.1).

3.1.1 The Orion Nebula Cluster

We also applied our estimate from numerical simulations to a real star cluster – the ONC. This young star cluster consists of all stars from the O and B classes down to the H-burning limit and brown dwarfs. In order to compare it with our models, we compiled the most complete dataset from the past 30 years and more, from the X-ray, UV, visible, near-IR and IR wavelengths. The detailed discussion and methods of cross-correlating different catalogues are thoroughly described in (Pavlík et al. 2019). Here in Tab. 3.1, we include parameters of several sources to show the data structure. The whole table of sources is only available online[3].

In total, the ONC contains around 2400 sources and is, therefore, comparable to our model with 2.4k stars. In this model, the time required for the primordial mass segregation to vanish is $\langle\tau_{\rm v}\rangle \approx 8.4\,$Myr. The ONC, being only 2.5 Myr old, should, therefore, still show evidence for its primordial mass segregation if it formed in that way. We are aware that the ONC cannot be directly compared to a spherically symmetric N-body model, which is merely a mathematical representation of a star cluster. It contains three populations of stars (Beccari et al. 2017) and high initial binary population (Kroupa 1995; Kroupa et al. 2001; Belloni et al. 2017), large extinction in different wavelengths is measured (Scandariato et al. 2011) because of the obscure Orion molecular cloud (Hillenbrand 1997; Hillenbrand & Hartmann 1998), and its overall shape is elongated Hillenbrand & Hartmann (cf. 1998). Therefore, we have performed modifications to our model in order to satisfy the observational properties of the ONC. Our results suggest that the ONC is comparable to a cluster which formed completely mass segregated. Further investigation with asymmetric models containing gas and binary stars would, however, be convenient to support this claim.

3.2 Core collapse

Let us now turn back to the evolution of star clusters in general, mainly from a thermodynamical point of view. We have already mentioned that cluster evolution may be modelled to a certain degree of accuracy assuming an ideal gas. Using this analogy, we may assign the system a kinetic temperature, T, which is defined through the equation for kinetic energy

$$K = \frac{3}{2} N k_{\rm B} T\,, \tag{3.8}$$

[3]The electronic form is at the CDS via anonymous ftp to cdsarc.u-strasbg.fr (130.79.128.5) or via http://cdsweb.u-strasbg.fr/cgi-bin/qcat?J/A+A/626/A79

Table 3.1: Data of the ONC used in this work (taken from Pavlík et al. 2019). Column names and several lines are shown to demonstrate the data structure.

RA [°]	DEC [°]	[H97b]	[HC 2000]	[MLLA]	[FDM2003] Opt	[FDM2003] X	[FDM2003] X_2	[DRH 2012]	[COUP]	[PMF 2008]	M_{H97b}	M_{FDM2003}	M_{B98}	M_{DM98}
83.617...	−5.444...	1			22						0.11	0.15		
83.618...	−5.416...	2			23	8					0.67	1.20		
83.618...	−5.649...							1267					0.038	0.055
83.620...	−5.244...							784						0.700
83.776...	−5.519...	294			228						0.15	0.21		
83.776...	−5.411...	291	99	161	230	136					0.27	0.43		
83.803...	−5.345...	391	699	916	293	214	222				0.29	0.43		
83.857...	−5.493...	789									0.20			
83.709...	−5.442...								53					
83.807...	−5.359...		602	797					570	34				
...														

[H97b] is the Simbad identifier of the data from Hillenbrand (1997) with multiplicity index

[HC2000] is the Simbad identifier of the data from Hillenbrand & Carpenter (2000)

[MLLA] is the Simbad identifier of the data from Muench et al. (2002)

[FDM2003] is the Simbad identifier of the data from Flaccomio et al. (2003a,b), where Opt is for the optical, X is for the X-ray, and X_2 is the identifier of an additional X-ray source that was also cross-matched to the optical data

[DRH2012] is the Simbad identifier of the data from Da Rio et al. (2012)

[COUP] is the Simbad identifier of the data from Getman et al. (2005)

[PMF2008] is the Simbad identifier of the data from Prisinzano et al. (2008)

M_{H97b} is the mass given in Hillenbrand (1997)

M_{FDM2003} is the mass given in Flaccomio et al. (2003a,b)

M_{B98} is the mass given in Da Rio et al. (2012) from Baraffe et al. (1998)

M_{DM98} is the mass given in Da Rio et al. (2012) from D'Antona & Mazzitelli (1998)

where $k_{\rm B}$ is the Boltzmann constant. We may also define the heat capacity as a derivative of its total energy with respect to temperature

$$C = \frac{\mathrm{d}E}{\mathrm{d}T}\,. \tag{3.9}$$

Consequently, any finite self-gravitating system in virial equilibrium, i.e. a system for which

$$E = -K \tag{3.10}$$

is valid, will have negative heat capacity (Lynden-Bell & Wood 1968) and should contract as it becomes more bound. The region where the virial equilibrium applies is circumscribed by a sphere of radius $r_{\rm v}$ (the virial radius), e.g. a star cluster core makes a good representative of a system in virial equilibrium. Since the increase of binding energy (i.e. the loss of "heat" energy) induces further loss of energy, the cluster core should evolve in a finite time to a stage with infinite density and temperature (as it was derived for continuum models of star clusters). This stage is called the *gravothermal catastrophe* or *core collapse*.

In N-body simulations, however, a complete collapse is prevented due to the presence of tightly bound (hard) binary stars which interact with the surrounding stars and give them energy. They are acting as a heat agent, thus lowering the temperature of the core (e.g. Aarseth 1972; Hut 1983; Fujii & Portegies Zwart 2014; O'Leary et al. 2014). Nevertheless, the notion of time of core collapse is used even in the N-body framework (usually linked to the time when the core reaches its maximum density) and represents an evolutionary "milestone" for star clusters. Several other features of star clusters (even the observed ones) are also interpreted in the context of core collapse (e.g. their surface brightness profile and the formation of blue stragglers), although these systems are already much more complicated – they contain stars of various masses and ages, include stellar evolution etc., so the thermodynamical assumptions are no longer straightforwardly applicable. We note that just by using the point-mass approximation in a dense environment, such as a cluster core, we may actually extrapolate to the time of core collapse. As the stars are very close, their tides, which can dissipate the relative orbital kinetic energy, are no longer negligible and may speed up the collapse significantly, induce binary star formation or even coalescence (Binney & Tremaine 1994).

3.2.1 Self-similar evolution

According to Lynden-Bell & Eggleton (1980), the evolution of a spherically symmetric collisionless system prior to core collapse is self-similar. This means that the radial density profile of the whole cluster above a certain radius is given by a scale free power-law

$$\rho \propto r^{-a} \tag{3.11}$$

(cf. also Larson 1970). This is a result of different relaxation timescales in the core and halo. Stars in the cluster core tend toward a near-Maxwellian velocity distribution much more quickly. The core is stripped of rapidly moving stars (in the tail of this distribution) which then populate its halo, causing the core to

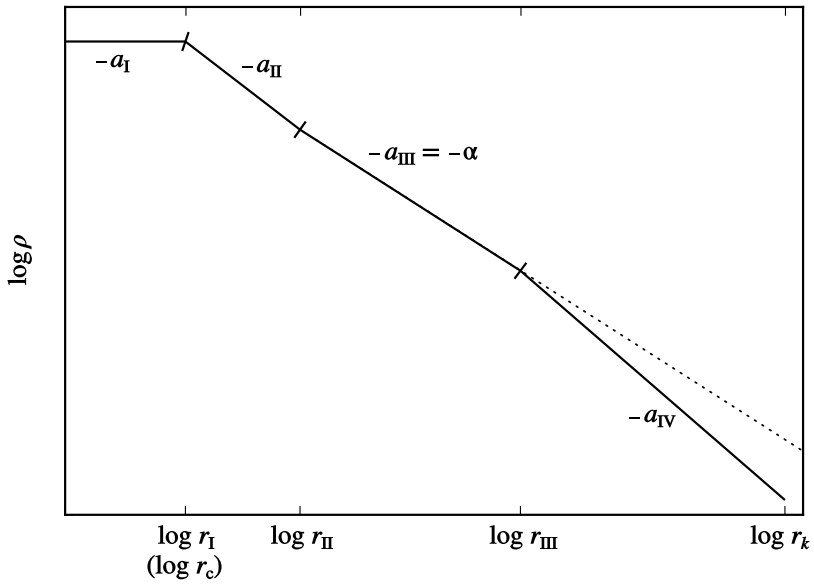

Figure 3.3: Schematic plot (taken from Pavlík & Šubr 2018) of the radial density profile in an analytical model and an N-body cluster prior to core collapse. Four different values of the logarithmic density gradient, $a_{\mathrm{I-IV}}$, are present. The dotted line is a continuation of the slope α and shows the asymptotic solution of Lynden-Bell & Eggleton (1980). The break radius r_{I} is identified with the core radius, r_{III} roughly corresponds to the half-mass radius, and r_k is the cluster radius (in an analytical model, the cluster extends to infinity and no break at r_{III} is present).

shrink and allowing it to relax even more quickly (Lynden-Bell & Eggleton 1980). After a certain period of time, the star cluster develops layers – an onion-like (i.e. self-similar) structure.

When the central density of an analytical model becomes infinite, the radial density profile of the whole cluster would be given by a single power-law with index $a = \alpha$. Before this moment, however, there is a composite power-law – the theoretical slopes are illustrated in Fig. 3.3 and are labelled as a_{I}, a_{II} and a_{III}, where the last one goes to α asymptotically. The core density profile is flat ($a_{\mathrm{I}} = 0$) and decreases outward. The core radius is represented in the figure by r_{I} or r_{c}. The slope does not reach α until a certain radius (denoted as r_{II}). As Lynden-Bell & Eggleton (1980) argue, if the slope is common for the whole system with a value α (in the extreme case of an infinite central density) but is flat (has a value of zero) in the core, due to the conservation of mass, a must have a higher absolute value than α in the region around the core (i.e. $a_{\mathrm{II}} \approx 2.4$). Their best fit for an analytical model is $\alpha \approx 2.21$ and the derived theoretical limits are $2 < \alpha < 2.5$.

Cohn (1980) and Takahashi (1995) derived $\alpha \approx 2.23$ for the asymptotic power-law slope using isotropic and anisotropic models in a Fokker–Planck approximation. Numerical N-body models (e.g. Giersz & Heggie 1994; Makino 1996; Baumgardt et al. 2003; Pavlík & Šubr 2018) show also a good agreement with the prediction of Lynden-Bell & Eggleton (1980) and provide values of α within their interval (between 2 and 2.5). However, there is one major difference – in

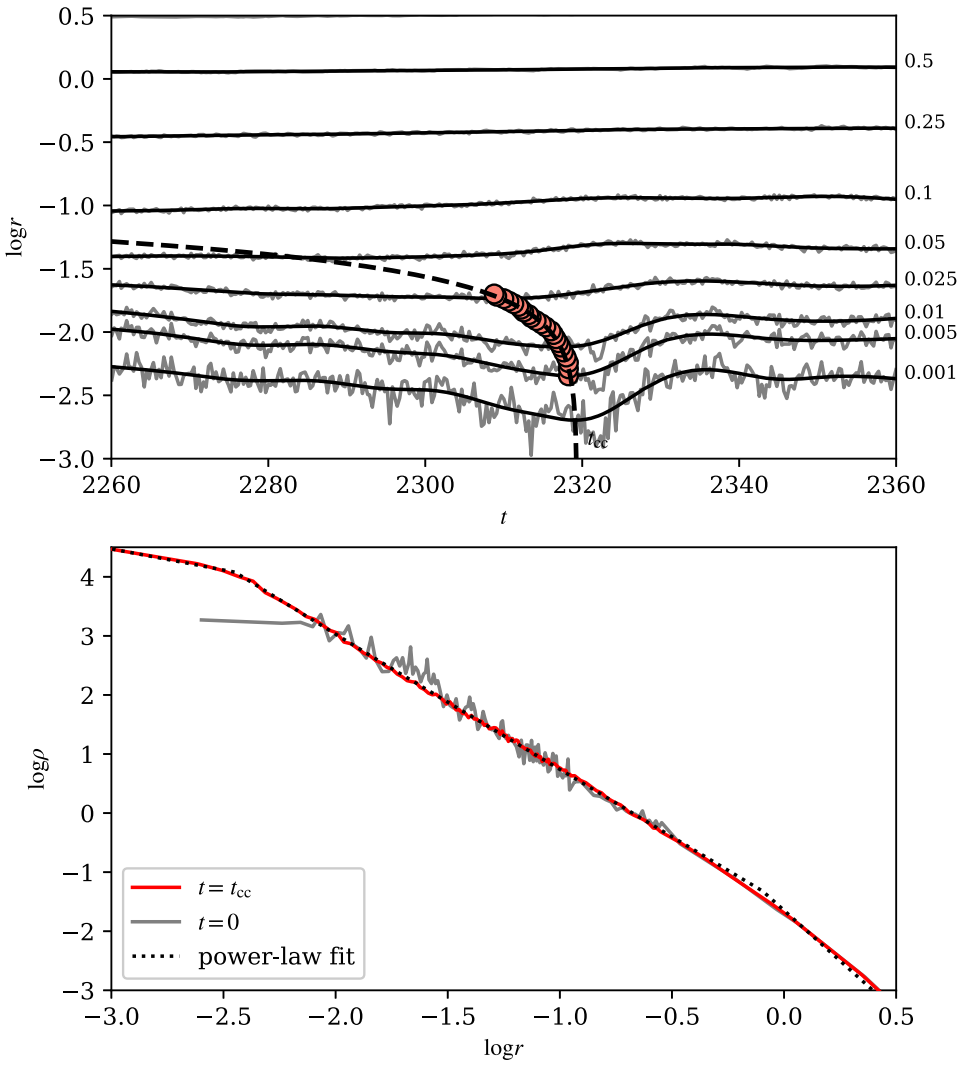

Figure 3.4: The top plot is a detail of the Lagrangian radii of one realisation of a model with 10k equal-mass stars and their evolution in time (expressed in Hénon units). The output data (grey lines), with their mass fractions displayed on the right, are smoothed (black lines) to simplify finding of their minima (red circles). Due to a better visibility, not all the output data lines are shown. The dashed line is a power-law fit through the minima. The bottom plot shows radial density profiles of the initial conditions (grey line) and at the moment of core collapse, t_{cc} (red line). The dotted line demonstrates a fit through the data. (taken from Pavlík & Šubr 2018)

an N-body system, the slope α is not asymptotic. As Spitzer & Hart (1971b) showed, the outer cluster halo tends again toward a Maxwellian velocity distribution on the relaxation timescale. This implies that the slope must diverge from the asymptotic value – their derived value is $a_{\mathrm{IV}} = 3.5$, see the notation in Fig. 3.3. Therefore, we fitted the radial density profile of our numerical models by a triple-broken power-law function. The results from a realisation of a model with 10k equal-mass stars and an initial Plummer density profile are plotted in Fig. 3.4. We also studied a larger model with 50k stars of equal masses and the same initial profile for comparison. In both of these models, our results agree

with all the previous assumptions and results, in particular $a_{\text{II}} \approx 2.4$, $a_{\text{III}} \approx 2.3$ and $a_{\text{IV}} \approx 3.4$ with a high level of accuracy (cf. Tabs. A.2 & A.3 in Pavlík & Šubr 2018). Moreover, we are able to conclude that the evolution of these models before the core collapse is self-similar as well because the value a_{III} from the radial density profile at the time of core collapse (see the lower panel of Fig. 3.4) has the same value as the power-law index α fitted to the minima of the Lagrangian radii (i.e. the radii of concentric spheres containing a fixed fraction of the total mass of the system; see the upper panel of the same figure). The dashed line fitted to the minima of the Lagrangian radii does also represent the boundary between the newly developed core and its halo. We note that this "self-similar" core should not be misinterpreted as the actual cluster core which is calculated in `nbody6`.

Using self-similarity, we developed a novel method to determine the time of core collapse and our results are consistent with other ways of seeking this time (e.g. from the minimum core radius, maximum core density, core bounce or the formation of the first hard binary star). An obvious issue concerns the core radial density profile. According to theoretical predictions based on the results from a continuum model, a_{I} should be zero. However, the discrete nature of N-body systems is inconsistent with this due to a finite number of stars present in the core – the radial profile may have a slightly positive or even negative slope which, however, does not contradict the self-similar evolution. Higher uncertainty of the central radial profile is, therefore, allowed (cf. Tab. A.3 in Pavlík & Šubr 2018).

3.2.2 The role of unequal masses

Up to now, we have investigated only the properties of isolated models with stars of equal masses. Among the N-body family, such models are the simplest ones imaginable and they are also seemingly similar to the continuum models. Aside from different techniques that are used to follow the evolution and obviously a distinct nature of the systems, the only major difference introduced into the calculations is discreteness. Although equal-mass clusters may be treated as star clusters, they are not something we would find among real objects. However, with the addition of "realness" into the numerical models (e.g. different masses of stars, stellar evolution, primordial binary fractions, interstellar medium or galactic potential), setting the initial conditions becomes very tedious, not straight forward and may grow out of control very fast. Models combining every aspect of real star clusters are called "kitchen sink" which is a very fitting name suggesting all the initial parameters to be mixed and flushed down the drain, making it very cumbersome to follow what is relevant for which part of the evolution and what is not. And still, even these models are merely a mathematical representation, not real star clusters. Investigating isolated equal-mass systems is, therefore, necessary to understand the nature of the problem and useful to do before we start exploring more complex models.

Having the results from equal-mass models already in agreement with earlier models and analytical predictions of the self-similar evolution, we increased the difficulty one step further by adding a single power-law IMF (Salpeter 1955). Two models were calculated (with 20k and 100k stars) to test our method for

finding the time of core collapse. As there are stars of different masses, the whole evolution is faster than in the case of equal-mass systems due to mass segregation. The encounters of stars are also more energetic, therefore, stars move faster (especially in the central regions) which makes, e.g., the Lagrangian radii more noisy (cf. Figs. A.1 to A.4 in Pavlík & Šubr 2018). Establishing the time of core collapse rendered more difficult which yielded in higher uncertainty (up to 15 %, whereas in the equal-mass models, the deviation was around 0.2 %). Nevertheless, we obtained consistent results within all realisations of each model. Moreover, the time of core collapse is again well correlated with the time of formation of the first hard binary star (with a correlation coefficient of about 0.58), which may also serve as a reliable indicator (Fujii & Portegies Zwart 2014). Binary stars will be discussed in more detail in the next chapter.

Within the uncertainties, even the models with unequal stellar masses seem to evolve self-similarly before the core collapse. The radial density profile at core collapse also seems to obey by the same rules which were discussed in the analytical case of Lynden-Bell & Eggleton (1980) or the equal-mass model in Sect. 3.2, i.e. the slopes described in Fig. 3.3 are valid. However, the values of $a_{\mathrm{I}-\mathrm{IV}}$ and α are vastly different from the previous case. In particular $a_{\mathrm{I}} \approx 0$, $a_{\mathrm{II}} \approx 1.8-2.1$, $\alpha \approx a_{\mathrm{III}} \approx 1.5-1.6$ and $a_{\mathrm{IV}} \approx 4$ (cf. Tab. A.3 in Pavlík & Šubr 2018). Nonetheless, a higher deviation and even different values of the slopes were expected since the introduced IMF placed these models farther from the analytical prediction than the equal-mass models.

4. Sub-system evolution

"Big doors swing on little hinges."

— an old proverb

The evolution of star clusters goes hand-in-hand with the evolution of systems that it contains within. We have already seen that massive stars are responsible for mass segregation and may speed up the cluster's evolution. The cluster's evolution may be also sped up by introducing some fraction of primordial binary stars. And finally, the presence of hard binary stars is able to stop the core from collapsing and sustain the cluster.

4.1 Binary stars

Observations show that at least 40 to 50 % of stars at present have a stellar companion (Duquennoy & Mayor 1991; Raghavan et al. 2010; Tokovinin 2014a,b). The observations of pre-main sequence objects show that stars are more likely to born in pairs, which has also corroborated numerical simulations (cf. Kroupa 1995; Kroupa et al. 2001; Belloni et al. 2017). The formation of very tightly bound (i.e. hard) binaries is thought to occur through two channels. In one, the binary is primordial, meaning that two stars were already born in a pair when the star cluster formed. Among these, the tightly bound ones would go through several interactions with other stars and harden over time (e.g. McMillan et al. 1991, and citations therein). Alternatively, a binary system may form dynamically, which is our focus here.

If we follow the argument of self-similar evolution of a cluster from the previous chapter further in time, at some point, the cluster core should consist of just a small number of bound stars. It is, therefore, expected that a tightly bound (hard) binary will form there dynamically. But the formation process remains uncertain. Some studies predict a sequence of consecutive three-body encounters that harden the system (Hills 1975; Heggie 1975). In contrast, more recent studies by Tanikawa et al. (2012, 2013) illustrate the complexities in a real cluster core with a fluctuating background density. They find that more than three stars must interact and the binary emerges as a result of a chaotic and very rapid interaction among them. Geller & Leigh (2015) showed that in an open cluster, three-body (binary and single star) or four-body (two binaries) encounters are – in at least 20 to 40 % of the cases – interrupted by interaction with another star. Instead of a nearly isolated few-body interaction, which is more typical in larger

systems (e.g. globular clusters), stars in the less populous systems interact and exchange energy in a group of stars in the cluster core. Nonetheless, whatever the process for exchanging binding energy is, the formation of the first hard binary is inevitable if the cluster is going through a core collapse.

If a binary forms (or hardens) in a collapsing cluster core, it acquires binding energy, $E_{\rm bin}$, of the same order as the core itself. As the core shrinks, the cross-section of three- or multi-body interactions of this hard binary and other stars grows and makes such a binary star act as a heat source, thus cooling the core and preventing it from collapsing further (e.g. Aarseth 1972; Hut 1983; Rasio et al. 2001; Fujii & Portegies Zwart 2014; O'Leary et al. 2014). Once a binary star becomes sufficiently bound, i.e. its binding energy exceeds several $k_{\rm B}T$, where $k_{\rm B}$ is the Boltzmann constant and T is the kinetic temperature, see Eq. (3.8), it has a very low probability of being destroyed (Heggie 1975) and in a constant background density such a system may even be "immortal" Goodman & Hut (1993). This energy relates to N-body variables (in Hénon units) by

$$1\,k_{\rm B}T = \frac{1}{6N}\,, \tag{4.1}$$

where N is the total number of stars. The binding energy of several $k_{\rm B}T$ (sometimes even tens or hundreds of $k_{\rm B}T$) is only obtainable in a dense environment, e.g. a collapsing core. We thus expect that the time of the first appearance of a hard binary is correlated with the time of core collapse and that its binding energy – or the multiple of $k_{\rm B}T$ – strongly depends on the potential well that formed it, i.e. on the size and mass of the core (as investigated, e.g., by Fujii & Portegies Zwart 2014; Pavlík & Šubr 2018). We have found that in an equal-mass star cluster with 10k stars, the binding energy of the first hard binary to appear during the core collapse, is 10 to $100\,k_{\rm B}T$, but the energy flow into binaries was detected even up to $10^3\,k_{\rm B}T$. In more populous clusters, e.g. containing 50k stars, $E_{\rm bin}$ of the first such binary is around $10^3\,k_{\rm B}T$ (cf. Tab. A.1 and Figs. A.10 & A.11 in Pavlík & Šubr 2018).

After core collapse, this hard binary system can be (and often is) ejected from the core by an energetic three-body interaction. In larger systems, such as a 50k star cluster, the core may then recollapse and the whole process repeats. These periods of collapse and binary ejection lead to core pulsations – oscillations of the core radius – as first discussed by Makino (1996). Energy is removed at the end of each collapse; hence, a less extreme collapse is expected. Using equal-mass cluster models, we have found that even these subsequent collapses exhibit self-similar properties along with the first core collapse (Pavlík & Šubr 2018).

4.2 Stellar evolution

Assuming that stars are unchanging point masses is the easiest one to adopt when seeking to understand the essential features of star cluster dynamical evolution. Despite its simplicity, which may seem very far from what we would consider a real cluster, we can appropriately analyse some important evolutionary features (e.g. the link between the core collapse and the formation of binary stars). There

are, however, cases where such an approach must be insufficient. One of them concerns the effects of stellar evolution.

Combining N-body calculations with detailed stellar evolutionary models raises the complexity (and cost) of such simulations enormously. Instead, a simpler and effective approach suggests itself – stellar evolutionary models are calculated beforehand and then implemented via parametric algorithms (e.g. Hurley et al. 2000, 2002)[1], which contain tables for mass-loss or gain ($\mathrm{d}m/\mathrm{d}t$) based on the epoch and consequently determine the actual stellar type of the star. Evolution of a star depends on its mass, so an IMF must be also introduced in these N-body simulations. The limitation now is that masses generated by the IMF must be compliant with the stellar evolutionary models (as is, e.g., Kroupa 2001). For the purpose of numerical modelling, we can continue to use the point-mass approximation since the stellar separations are large. Along with mass and components of the position and velocity vectors, each body is also assigned a parameter value defining its stellar type in the output.

Single-star evolution and the algorithms of Hurley et al. (2000) depend only on mass and metallicity of a body – more massive stars evolve faster, and lower metallicity induces a lower mass limit for the stellar core collapse and speeds up a possible supernova (SN) explosion with a consequent neutron star (NS) or black hole (BH) formation. Assuming, for instance, the average metallicity of stars in globular clusters in the Galaxy – i.e. $Z = 0.05$ or $[\mathrm{Fe/H}] = -1.3$ (as derived by Baumgardt & Sollima 2017) – an optimally sampled Kroupa IMF (Kroupa 2001; Kroupa et al. 2013) from 0.1 to 100 $M_\odot$, and only single-star evolution (Hurley et al. 2000), the last SN that produces a BH explodes at approximately 11.7 Myr (Pavlík et al. 2018). The progenitors of NSs are less massive, so the last NS under these conditions will form around 60 Myr. With the introduction of binary stars, the evolution gets more complicated because of possible mass transfer, accretion, or coalescence (see, e.g., Hurley et al. 2002). Eventually, this may even lead to delayed SN explosions of massive stars, as studied by Podsiadlowski et al. (1992) and De Donder & Vanbeveren (2003), or more recently by Zapartas et al. (2017).

4.2.1 Neutron stars

According to the currently understood scenario (Hurley et al. 2000), a main sequence progenitor star must have between 9 and 20 $M_\odot$ to possess sufficiently massive core to exceed the Chandrasekhar limit at the end of its life to explode as a core collapse SN and to form a NS, but not a BH. Massive star clusters (e.g. globular) are optimal environments for birthing a substantial population of NSs – and thus possible X-ray sources – since they contain a wide range of massive stars (Fabian et al. 1975). Bahramian et al. (2013) found a direct correlation between the number of X-ray and radio sources, and the stellar encounter rate

$$\Gamma \propto \frac{\rho_\mathrm{c}^2 r_\mathrm{c}^3}{\sigma}\,, \tag{4.2}$$

[1] Recently, new improved algorithms have been introduced that are in better agreement with observations, e.g. the masses of black hole mergers (Belczynski et al. 2010, 2016). These were not used in this work, however, but their influence on our results is discussed, e.g., in Pavlík et al. (2018).

where ρ_c is the core density, r_c is the core radius and σ is the velocity dispersion. Due to their high stellar densities and relatively low velocity dispersion, Γ reaches higher values in globular clusters than in other, less massive and less populous, stellar systems.

There are two ways of forming a NS: (i) type-II SN explosion of a massive star (i.e. a core collapse SN) or (ii) electron-capture supernova (ECS; Podsiadlowski et al. 2004, cf. also Katz 1975). Most of the NSs that form within the cluster after a SN II are not retained. Due to an asymmetry in the SN explosion and the conservation of momentum, the newly formed NS receives a natal *velocity kick*. The best fit kick velocity distribution from the observed Galactic pulsars seems to be Maxwellian with a dispersion of $\sigma_{\rm NS} \approx 190\,{\rm km\,s^{-1}}$ (Hansen & Phinney 1997) or even $\sigma_{\rm NS} \approx 300\,{\rm km\,s^{-1}}$ (Hobbs et al. 2005). In either case, this far exceeds the required velocity to escape from the cluster's gravitational potential well and most of these NSs escape in the field (Davies & Hansen 1998; Trenti et al. 2010). NSs that form by ECS receive little or no kick because of the very small asymmetry in neutrino emission (Gessner & Janka 2018).

Those NSs that remain in the cluster (i.e. those who received only a small or no kick) due to mass segregation naturally sink towards its core where they may form binaries (either a NS with a star, with another NS or with a BH) through close interaction of two or three stars or tidal capture (e.g. Hut et al. 1992; Banerjee & Ghosh 2007). Tidal capture seems to be the most efficient in producing tight binary systems (Fabian et al. 1975). Binaries with two NSs may be observed as millisecond pulsars (MSPs) or as low-mass X-ray binaries (LMXBs). Their typical X-ray and γ-ray luminosity is from 10^{31} to $10^{38}\,{\rm erg\,s^{-1}}$ (e.g. Ivanova et al. 2008). The process of formation of a MSP is complex and not yet fully understood (cf. Tauris 2011). However, it has been argued, and commonly accepted, that the spin-up of a NS to periods of milliseconds happens in binaries due to the accretion of material from a Roche lobe overflowing companion star (Alpar et al. 1982; Phinney & Kulkarni 1994). The fraction of spun-up NSs was found to be around 10 % (Abbate et al. 2018). We note that the NS reaches the fastest spin long before becoming unstable to gravitational wave emission due to non-radial stellar modes (Papaloizou & Pringle 1978). This process, during which the NS is observable in X-ray, can last up to 10^8 or $10^9\,{\rm yr}$ (Fabian et al. 1983; Tauris et al. 2012).

4.2.2 Black holes

Recent observational and numerical results of Peuten et al. (2016) and Baumgardt & Sollima (2017) predict at most 50% retention of BHs in the present day Galactic globular clusters (GCs). This is a product of long dynamical evolution that lasts billions of years. These studies did not, however, constrain the initial fraction of BHs. To address this, we set up and analysed hundreds of numerical models of star clusters with different initial conditions to draw conclusions on the initial retention fraction of BHs, which is affected mostly by the natal SN velocity kicks and only slightly by dynamical effects (Pavlík et al. 2018). We note that only the core collapse SNe were considered in this work.

Two important results were found for compact clusters with a small number of stars (i.e. $r_{\rm h} = 0.5\,{\rm pc}$ and $N = 10^3$):

(i) Since the IMF is optimally sampled and the stellar evolutionary models are known, we can predict the number of BHs that are supposed to form. However, in these compact star clusters, there is an overproduction of BHs compared to the expectation from the used IMF. In the left panels of Fig. 4.1, we plot the mean fraction of BHs that formed in each of the investigated models. The most compact and smallest system has about 50% excess relative to other models.

(ii) The evolutionary tables for single-star evolution should give exactly the same results for a given mass and metallicity everywhere in any model. However, there is a systematic delay of SN explosions in the most compact and least populous cluster models. The last SN forming a BH is delayed from the predicted 11.7 Myr by up to 15 Myr (compare the results in the middle panels of Fig. 4.1).

Both of these results are due to binary-stellar evolution. Stars in pairs may exchange mass with their companion and consequently rejuvenate themselves while the companion grows to so high a mass that it produces a BH instead of its former fate (e.g. becoming a NS). To support this claim, we show the mean time that a star that produces a BH spent in a binary star, see Fig. 4.1. There is a clear difference between the most compact and least massive cluster and the rest of the models.

In the models, the assumption was that SN kicks for BHs are the same as for NSs. By varying the parameters of these kicks, i.e. the three-dimensional Gaussian kick velocity dispersion[2] $\sigma_{\rm BH}$, we conclude that to satisfy the observational constraints, the mechanics of a velocity kick for a BH must differ from a NS. Either there is a greater impact of the fall-back mass onto the remnant, which reduces its speed, and thus effectively lowers the magnitude of the kick velocity dispersion, or there is a bimodal distribution (as proposed by Verbunt et al. 2017). If the mass of the host cluster is higher, which means a deeper potential well and higher escape velocity, $\sigma_{\rm BH}$ could also be greater.

We have also developed a simple analytic estimate for the BH retention fraction (cf. Sect. 3.2 in Pavlík et al. 2018) which corroborated our N-body models in the simulated range of cluster masses. We extrapolated the model to the mass range of globular clusters ($\sim 10^6\,M_\odot$) and up to the size of ultra-compact dwarf galaxies ($\sim 10^9\,M_\odot$). We propose that for BHs to achieve the same magnitude of velocity kick as NSs (as argued, e.g., by Jonker & Nelemans 2004; Repetto et al. 2012) which means $\sigma_{\rm BH} \approx 190\,{\rm km\,s^{-1}}$ (Hansen & Phinney 1997) or even $\sigma_{\rm BH} \approx 300\,{\rm km\,s^{-1}}$ (Hobbs et al. 2005), we would need a very dense environment comparable to a nuclear cluster (cf. Banerjee 2017, 2018). Only such a system has sufficiently deep potential well and high escape velocity that it would be able to retain enough BHs initially, so that after billions of years of dynamical evolution, the number of remaining BHs would be in accordance with the observations (Peuten et al. 2016; Baumgardt & Sollima 2017).

[2]This is equivalent to a Maxwellian distribution fitted to the observed NSs.

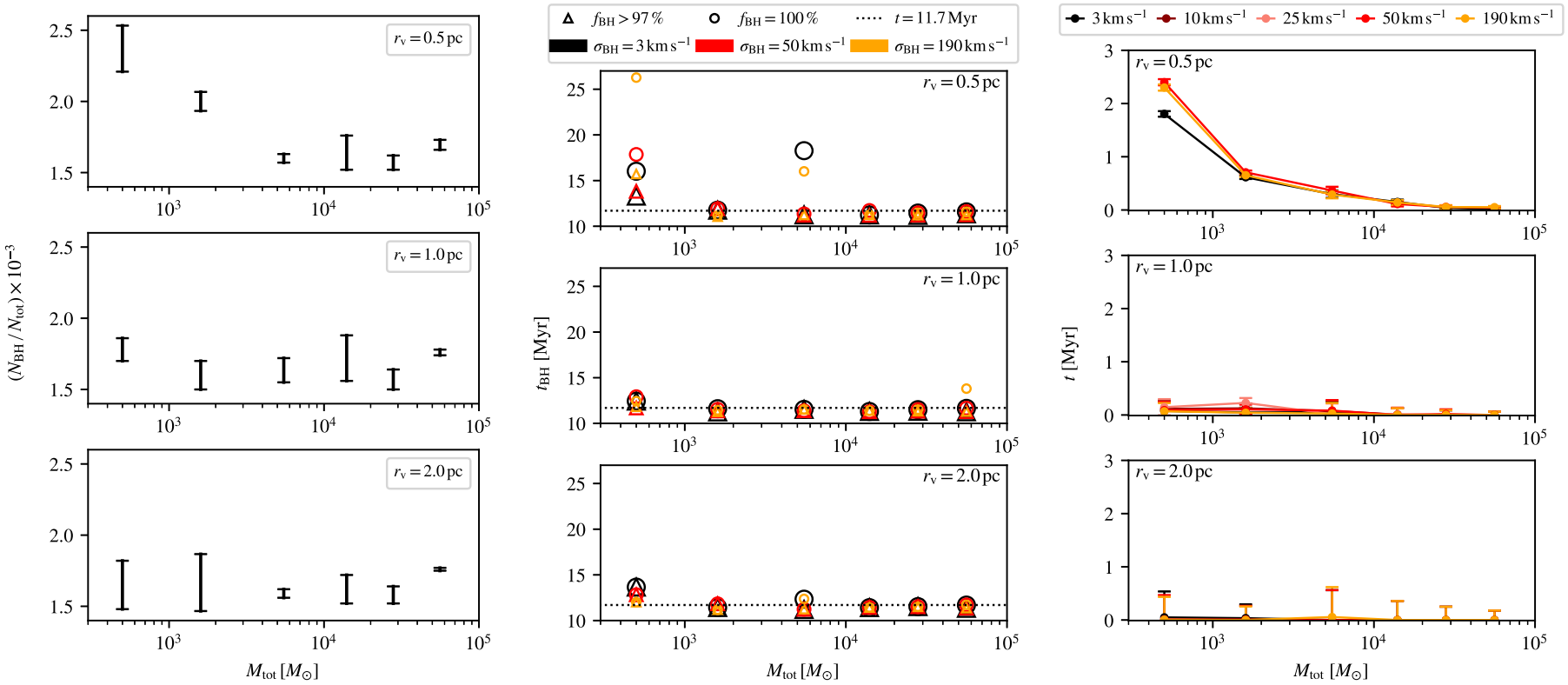

Figure 4.1: As a function of the total initial mass of a star cluster, we show the mean fraction of BHs that formed in the investigated models (left panels), the time when 97 % and 100 % of BHs formed (middle panels), and the mean time which BH progenitors spent in binary stars (right panels). Three different sizes of clusters were considered for each mass: $r_v = 0.5$, 1.0 and 2.0 pc. Five different values of the velocity kick dispersion were analysed: from $\sigma_{BH} = 3$ to 190 $km\,s^{-1}$. (taken from Pavlík et al. 2018)

The presence of BHs in the cluster is important for a possible formation of BH–BH binaries and a possible growth of an intermediate-mass BH (IMBH; recently, e.g., Arca-Sedda & Capuzzo-Dolcetta 2018; Šubr et al. 2019, and references therein) whose existence has not yet been proven, although candidates for the host clusters, e.g. ω Cen or 47 Tuc, are heavily debated (cf. Anderson & van der Marel 2010; van der Marel & Anderson 2010; Noyola et al. 2010; Jalali et al. 2012; Baumgardt 2017; Kızıltan et al. 2017; Zocchi et al. 2017, 2019). Later phases of this gradual merging of BHs into an intermediate-mass object would be detectable by the upcoming *LISA*[3] mission as intermediate-mass ratio inspirals (IMRIs; as discussed in the ASTRO-GR meeting, 2018; or see, e.g., Amaro-Seoane 2018). Hence, both numerical and observational approaches in this field are desired.

Stellar BHs are also responsible for the evolution of the cluster stellar population. Dynamical friction influences BH progenitors and BHs more than other stars due to their superior masses, so they naturally sink towards the cluster core sooner. The effect of dynamical friction on less massive bodies (e.g. NSs) is, therefore, reduced because of the smaller encounter cross sections. When BHs explode as SNe, their count in the cluster decreases due to kicks which may further lower the encounter rates. But another very important effect acts against mass segregation of less massive bodies. As we present in Fragione, Pavlík, & Banerjee (2018b, hereafter FPB18), when BHs are populating the cluster core, they behave like a dynamical heating engine and under their influence the NS population may even expand (see, e.g., Figs. 2 & 3 in FPB18). Further contraction of the NSs is restarted only when a majority of BHs is dynamically ejected from the core and their heating efficiency decreases; this can take up to several Gyrs.

In FPB18, we investigate how different metallicities of stars (i.e. $Z = 0.001$, 0.005 and 0.02) affect the results. Low metallicity massive stars lose much less matter, thus the BHs may be both more massive and more numerous, even for an identically sampled IMF. This produces higher kinetic energy in the rest of the cluster members. Consequently, the expansion of the NS population happens faster and the re-collapse occurs later.

Recent *LIGO*[4] gravitational wave observations detected the merging of BH–BH binaries which were in the field rather than in a star cluster (cf. Ziosi et al. 2014; Rodriguez et al. 2016, and citations therein). It is very unlikely that a BH–BH binary will escape directly after a kick. First, a single SN cannot eject both companions from the cluster. Second, there is no guarantee that both BH progenitors, which can form a binary, explode as a SN at the same time, so the only possible outcomes are that (i) the newly formed BH stays in the pair, or (ii) the binary breaks apart. Third, even if both stars exploded at the same moment and did not separate, it is virtually impossible that both would receive a recoil velocity kick in the same direction out of the cluster and stay bound. BHs that fail to escape from the cluster after a kick sink to the core where they dynamically form binary or multiple systems. Then, due to an energetic three-body interaction, such a BH–BH pair could be ejected from the star cluster core to either reside in its halo or populate the Galactic field (e.g. Sigurdsson & Hernquist 1993; Rodriguez et al. 2016, and citations therein). These field BHs will merge

[3]Laser Interferometer Space Antenna

[4]Laser Interferometer Gravitational-Wave Observatory

within the Hubble time (Ziosi et al. 2014) with a predicted rate of gravitational wave sources $1.6 \times 10^{-7}\,\mathrm{yr}^{-1}\,\mathrm{Mpc}^{-3}$ (Portegies Zwart & McMillan 2000). Understanding the BH retention in star clusters is, therefore, important for this channel of gravitational wave sources and this topic deserves further investigation in the future.

5. Galactic scale

Our Galaxy is classified as a barred spiral galaxy, composed of a disk with spiral arms, central bulge with a bar and a spherical halo. The disk is made up of stars, diffuse gas and molecular clouds, OB associations and young star clusters (sometimes referred to as open clusters). In the heart of the bulge lies a supermassive BH (SMBH) surrounded by a cluster of stars. The halo contains the oldest globular clusters (GCs; 150 of them are known, Harris 1996). Large nuclear and globular clusters are also present in elliptical and irregular galaxies and young star-forming clusters and associations are known in irregular or small galaxies, such as the Milky Way (MW) Galaxy satellites – the Small and Large Magellanic Clouds. Hence, clusters are, rightfully, considered to be the building blocks of galaxies.

5.1 Tidal field

A star residing within in a cluster that orbits in a galaxy feels not only the cluster's self-gravity but also the gravitational field of the host galaxy[1]. The region where the influence of the cluster is dominant for a cluster on a circular orbit is roughly delimited by the tidal radius.

$$r_{\rm t} = r_{\rm G} \left(\frac{M_{\rm c}}{3M_{\rm G}} \right)^{\frac{1}{3}} , \tag{5.1}$$

where $M_{\rm c}$ is the mass of the cluster within this radius, $r_{\rm G}$ is the distance of the cluster to the centre of the galaxy and $M_{\rm G}$ is the mass of the galaxy within the radius $r_{\rm G}$ (e.g. Spitzer 1987; Binney & Tremaine 1994). Assuming, e.g., our Galaxy, the cumulative mass up to a distance of $r_{\rm G} = 5\,{\rm kpc}$ is $M_{\rm G} \approx 5 \times 10^{10}\,M_{\odot}$ (Faber & Gallagher 1979; Bland-Hawthorn & Gerhard 2016). We note that Eq. (5.1) is the same as the Roche surface for the cluster, given the possibility of rotation of the cluster and density gradients within the system.

Beyond the tidal radius, stars predominantly feel the gravitational field of the galaxy and tidal tails of stars may develop. Stripping of stars from a cluster in a galaxy depends on many parameters (e.g. elongation and inclination of the cluster's orbit, rotation) and the limit given by Eq. (5.1) does not strictly hold. Stars stripped from the cluster populate the galactic disk, for instance, as in the case of Palomar 5 cluster (Dehnen et al. 2004). On the timescale of Gyr, galactic tides can also completely dissolve the cluster. Developing significant tidal

[1] In this case, the lowercase "g" indicates a generic galaxy, not only the Milky Way.

tails due to evaporation of stars takes hundreds of millions of years (e.g. Küpper et al. 2008), but early gas expulsion can, in principle, speed up this process. As Dinnbier & Kroupa (2019) argue, tidal tails may be found even for young Pleiades-like clusters which are only about 100 Myr old (Kroupa et al. 2001). They also predict the effects for systems observable by the *GAIA*[2] mission. Tidal forces are, however, not the only way that a cluster contributes stars to the galactic field population. Close few-body interactions (usually with two or three interacting stars) can eject single (or even binary) stars from the cluster. Such may be the channel for inserting NS–NS or BH–BH binaries into the field population, that are the sources of *LIGO* or *Virgo* gravitational wave signals, as we discussed in the previous chapter.

5.2 Millisecond pulsars

Observations by the *Fermi–LAT*[3] (Atwood et al. 2009) show a γ-ray excess around the Galactic centre with a diffused luminosity of the order of $10^{37}\,\mathrm{erg\,s^{-1}}$, extending up to 20°, with a peak at approximately 2 GeV and an almost spherical radial density profile $\rho \propto r^{-2.4}$ (Abazajian et al. 2014; Calore et al. 2015). The origin for this emission is not yet understood, but two hypotheses are current: dark matter annihilation emission (Calore et al. 2015) or emission from thousands of MSPs present near the galactic centre (e.g. Brandt & Kocsis 2015; Arca-Sedda et al. 2018; Fragione et al. 2018a; FPB18).

In FPB18, we show that GCs contain a large fraction of NSs (progenitors of MSPs). GCs within a galaxy behave like stars within a star cluster. They also sustain two-body relaxation as a population and experience dynamical friction (see Sect. 3.1), yet on a much longer timescale than the lower mass case (e.g. on the order of Gyr). As they are more massive than any other objects in the galaxy, with the exception of the central SMBH, they should spiral toward the galactic centre where they tidally disrupt and deposit their constituent stars – along with their NSs (Brandt & Kocsis 2015). Fragione et al. (2018a) found a log-linear relation between the observed γ-ray luminosity, L_γ (from 10^{31} to $10^{36}\,\mathrm{erg\,s^{-1}}$), and the globular cluster mass, M, based on the data from Hooper & Linden (2016)

$$\log \frac{L_\gamma}{M} = 32.66 \pm 0.06 - (0.63 \pm 0.11) \log M\,, \tag{5.2}$$

cf. Eq. (4) in FPB18. After applying the mean γ-ray emission $L_\gamma = 2\times10^{33}\,\mathrm{erg\,s^{-1}}$ (Brandt & Kocsis 2015), and the 10 % fraction of NSs that can become MSPs to our numerical models, we obtained an agreement with Eq. (5.2) to within 1σ, see the coloured points in Fig. 5.1. Our simulations, consequently, support the MSP origin of the galactic centre γ-ray excess.

Our Galaxy is not the only one with such a γ-ray excess, the Andromeda galaxy has a reported γ-ray emission of even one order of magnitude larger, with the measured diffused luminosity approximately $2.8 \times 10^{38}\,\mathrm{erg\,s^{-1}}$, and the excess extends up to 5 kpc from the Andromeda galaxy centre (Ackermann et al. 2012,

[2]Global Astrometric Interferometer for Astrophysics
[3]Large Area Telescope on board the *Fermi* Gamma-Ray Space Telescope

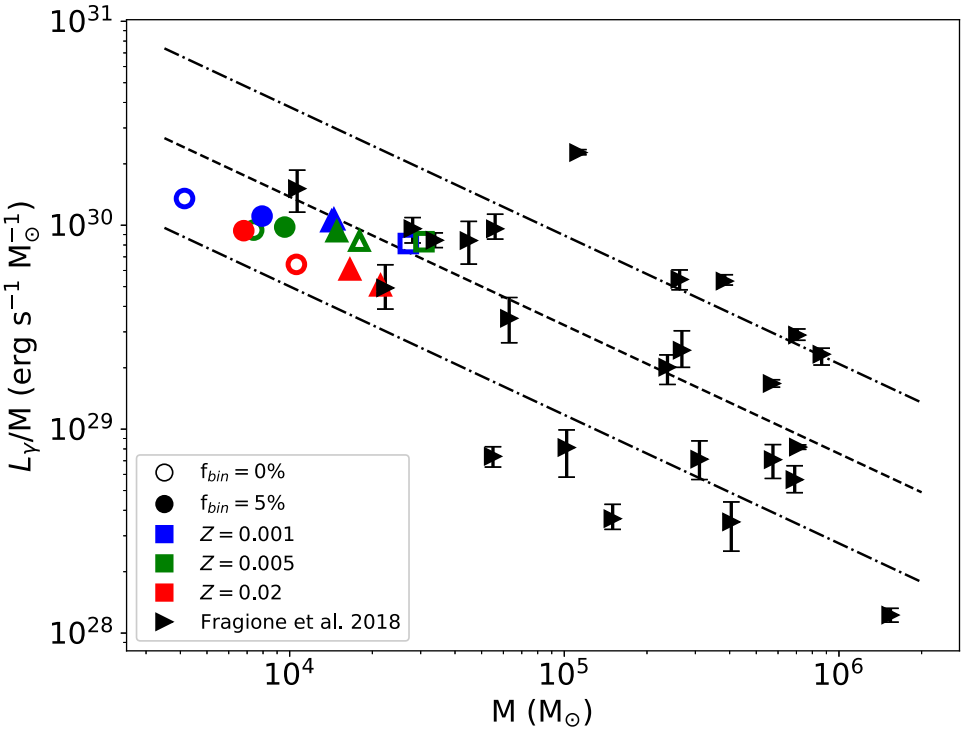

Figure 5.1: Ratio of γ-ray luminosity to globular cluster mass (L_γ/M) as a function of the cluster mass. The coloured symbols represent the inferred L_γ/M from the modelled globular clusters – various initial cluster masses were assumed (circles: $M_{\rm ini} = 3.0 \times 10^4 M_\odot$; triangles: $M_{\rm ini} = 5.0 \times 10^4 M_\odot$; squares: $M_{\rm ini} = 7.5 \times 10^4 M_\odot$). The dashed line shows the best log-linear fit from Eq. (5.2) and the dashdotted lines show 1σ deviations. (taken from FPB18)

2017; Eckner et al. 2018). Again, both MSPs and dark matter annihilation could play a role here (McDaniel et al. 2018), while higher mass of this galaxy compared to the MW means that there could have been more GCs which deposited larger number of NSs in the bulge and could have enhanced the γ-ray emission by a factor of 4 to 10 (Ackermann et al. 2017). Also the population of NSs which formed directly in the bulge may be responsible for up to $7 \times 10^{37}\,{\rm erg\,s^{-1}}$ (Eckner et al. 2018). Fragione et al. (2019a) used a semi-analytic model to simulate the primordial population of GCs in the Andromeda galaxy (cf. Gnedin et al. 2014). Their result is, however, approximately eight times lower than what is measured. Even after accounting for a burst of star formation and the subsequent increase of close binaries, the same mechanisms which is in agreement in the case of the MW Galaxy, cannot reliably explain what is going on in the core of Andromeda. Other sources of γ radiation seem to be required and further investigation of this problem is desired.

6. Discussion and perspectives of future research

"It is often the case in science that by solving one mystery another one appears."

— common wisdom

Due to the collaborative effort of Varri et al. (2018), the current state of knowledge about star clusters, stellar evolution, numerical codes and instrumentation or impact on future missions (e.g. *LISA*), as presented at the MODEST-17 conference[1], has been summarised. Many open questions are presented but at the same time certain areas that merit further investigation are proposed. The work presented in this thesis also uncovered a number of potentially fruitful areas for future investigation, a selection of which is presented below.

6.1 Core collapse

Self-similar evolution is not only a property of a spherically symmetric collisionless system (Lynden-Bell & Eggleton 1980), but is present even in equal-mass N-body models. This motivated us investigate whether it occurs in models with an IMF (Pavlík & Šubr 2018). The current results have, however, very high uncertainties and the effect is not as pronounced as in the equal-mass models. Contractions of the core region are shallower and, therefore, we cannot see clear sequences of the minima of Lagrangian radii as we do in the equal-mass clusters. These minima are key, in our method, for pinpointing the time of core collapse. We expect that larger models, extended at least by a factor of ten in stellar population may be needed to deepen the potential well substantially to produce a sufficiently deep core collapse. Such numerical studies are, however, very expensive and time consuming.

Furthermore, our models do not have any primordial binaries, so the appearance of the first hard binary star in each cluster is a good indicator of the time of core collapse (cf. Fujii & Portegies Zwart 2014). Analysing the effect of a primordial binary population on a binary star that emerges from the core collapse would be interesting. The processes leading to binary formation under such conditions would also be important for evaluating the role of binaries in the subsequent

[1] Modelling and Observing Dense Stellar Systems

collapses (or post-collapse oscillations). This is because after the star cluster has collapsed once, neither the formation of a new binary nor a large transfer of binding energy into an existing binary star can be used as a straightforward and reliable indicator of another collapse.

6.2 Binary star formation

Hard binary stars are important in the evolution of star clusters, especially when the cluster is going through a core collapse (e.g. Aarseth 1972; Hut 1983; Fujii & Portegies Zwart 2014; O'Leary et al. 2014; Pavlík & Šubr 2018). That is because three-body interactions (a binary star and an incoming star) are able to increase the dissolution rate of a star cluster, cool the core and prevent a complete collapse. According to Hills (1975) and Heggie (1975), after a three-body interaction, a softly bound binary is likely not to survive while, in contrast, a hard binary should acquire more binding energy. This process of hardening is supposed to be rather slow and consecutive although Tanikawa et al. (2012, 2013) argue that the process of hard binary formation is rapid and chaotic.

Binary formation in our models involves multiple stars, in some cases even simultaneously. The process also seems rather consecutive. For better statistics, we need a large sample of binary systems to obtain the duration of formation, energy balance and the number of stars involved. The issue is that each binary has a history of interactions and interchanging of components. Since there are two or more parents of each new binary star, the number of stars involved grows exponentially. If we count too many interactions, we may find that in a limit all stars in the cluster were involved in the formation of a single hard binary, which is obviously irrelevant. If we count too few interactions, the process of hardening may be underestimated. Deciding how far back we count or which interactions are relevant is quite difficult and, to date, unresolved.

6.3 Black hole retention

In the work on BH retention fraction (Pavlík et al. 2018), we introduce an analytic estimate for the number of BHs that should initially be retained in the cluster based on arguments about the density distribution of stars and the magnitude of the kick vs. the escape velocity at a given radius. Although this estimate is broadly in agreement with the results from our numerical simulations, it struggled fitting low-mass models that tend to be more influenced by stellar dynamics than more populous models. Improvements in the analytic model that would be able to include dynamical effects are needed. For instance, an escaping remnant should experience dynamical friction that should decelerate it and occasionally even prevent its escape from the cluster. Binary-stellar evolution also needs to be properly included because it may lower the kick velocity, produce more BHs, and/or delay the SN explosions.

The present models used older stellar evolution algorithms (Hurley et al. 2000, 2002) that cannot produce high-mass BHs. We know these exist and are the sources of recently observed gravitational wave events. Although we discuss the

effect of having larger BHs in our star clusters, improved calculations with newer algorithms (e.g. Belczynski et al. 2010, 2016) are highly desirable and should be included in the `nbody6` code (Aarseth 2003).

Another feature, that we did not consider but should certainly be modelled, is the fall-back of mass onto the remnant during the SN explosion. In our simulations, we omitted explicit fall-back because the current algorithm in `nbody6` scales the initial kick velocity, $v_{\rm kick,i}$, by the ratio between the mass of the envelope, $m_{\rm env}$, and the mass of the star before the SN explosion

$$v_{\rm kick} = v_{\rm kick,i} \frac{m_{\rm env}}{m_{\rm BH} + m_{\rm env}} \,, \tag{6.1}$$

where $m_{\rm BH}$ is the remnant's final mass. However, the mechanism that is responsible for the fall-back does not depend on the remnant's mass but only on the mass of the envelope which falls back. A recent theoretical derivation by Belczynski et al. (2008) suggests that the kick velocity scales with a fraction of the envelope mass, $\Delta m_{\rm env}$,

$$v_{\rm kick} = v_{\rm kick,i} \left(1 - \frac{\Delta m_{\rm env}}{m_{\rm env}} \right) . \tag{6.2}$$

The numerical approach should be extended to include this. Such a step would, however, need a physically well-motivated prescription for $\Delta m_{\rm env}$ for any given star.

6.4 Primordial mass segregation

The simulations performed in Pavlík et al. (2019) for evaluating primordial mass segregation in young star clusters are pure N-body, i.e. they do not include intracluster gas – a pure N-body integrator is not constructed for such a task. For a young embedded cluster (e.g. the ONC), the internal gas distribution plays a role in its global evolution. It has also been shown that the ONC is likely to contain three populations of stars (Beccari et al. 2017; Kroupa et al. 2018), whereas the models presented in Pavlík et al. (2019) have only a single population. Another issue with young open clusters is that they are formed in large filaments and tend to have a non-spherical shape on a large scale, whereas the numerical models used are spherical.

Although we have also attempted to model multiple populations, we were still limited by the requirement that the entire stellar population must be injected at once (i.e. merging the output of a smaller model with a new input). Gradual star formation is difficult and challenging to model with `nbody6`. It would, therefore, be interesting to focus on developing a more suitable tool, such as `AMUSE` (Portegies Zwart 2011), that could be used for modelling a complex star cluster with gas and an ongoing star formation.

6.5 Planetary systems

Ever since the first exoplanet's discovery (51 Peg b; Mayor & Queloz 1995) there has been an increasing interest in exoplanetary observations and analysis. It is a particularly fascinating topic in astronomy, not only for the prosaic reason of searching for extraterestrial intelligence (e.g. project *SETI*) but because we can learn how planetary systems form and evolve. At least there are now comparisons with our Solar System. Ground based observations are limited by our atmosphere and rotation of the Earth but the launch of dedicated satellites has opened a new era. The extraordinarily successful *Kepler* mission found thousands of exoplanets. New missions such as *TESS*[2], *CHEOPS*[3], *PLATO*[4] or *GAIA* are already operating in space or in preparation.

Although most stars are born in or live in binary or hierarchical systems, only about 3 % of all exoplanets have been found orbiting binary stars. A selection bias may play a role, but an important question is also raised about the stability of binary stars hosting a planet (Naoz et al. 2013; Wang et al. 2014; Thebault & Haghighipour 2015; Kraus et al. 2016; Fragione et al. 2019b; Fragione 2019). Having a planet on a stable orbit around one component of a binary star, not to say its birth under such conditions, is increasingly more difficult with the second companion in this binary closer to the host star (Haghighipour & Raymond 2007; Kaltenegger & Haghighipour 2013; Wang et al. 2014; Thebault & Haghighipour 2015). Because the companion exerts a gravitational tide, it can truncate any protoplanetary disk and reduce its mass (e.g. Miranda & Lai 2015), render it turbulent or dissipate it completely (Nelson 2000; Picogna & Marzari 2013). Even if planetesimals form, the companion may alter their accretion rate (e.g. Thébault et al. 2008), eccentricities, inclinations and collision rates, rendering it difficult for them to collide and form a full-fledged planet (Thébault et al. 2010; Xie et al. 2011; Marzari et al. 2012). Separation of the binary components of more than 50 au or close to 100 au is necessary to reduce the effect of the second star on the planet formation to a negligible level (Desidera & Barbieri 2007; Roell et al. 2012). Yet, several planets have been found in binaries with a separation as low as 3 to 5 au or $\lesssim 50$ au (Thebault & Haghighipour 2015)[5].

Dynamical exchange of stars (and planets) in binaries is common in dense stellar environments such as star clusters, especially when they approach the core collapse (Leigh & Geller 2013; Pavlík & Šubr 2018). It is, therefore, possible that planets which formed in wide binaries are later tightened dynamically (e.g. Pfahl & Muterspaugh 2006; Marzari & Barbieri 2007; Gong & Ji 2018). Pfahl & Muterspaugh (2006) were also the first to suggest the single–binary and binary–binary dynamical channel of planet formation in binaries. This channel of planetary formation has been studied numerically by Fragione et al. (2019b) and Fragione (2019). In a recent work (Pavlik & Fragione, in prep.), we are aiming to extend these studies by performing binary–binary scattering and analyse the subsequent stability of planets in binary star systems.

[2]Transiting Exoplanet Survey Satellite (Ricker et al. 2015)
[3]CHaracterising ExOPlanets Satellite
[4]PLAnetary Transits and Oscillations of stars
[5]http://exoplanet.eu/planets_binary/, from July 2018

6.6 Galaxy formation

Galactic GCs may reveal more than just the origin of the MSP population near its core. These objects can be also used to deepen our understanding of the formation and early evolution of our Galaxy – whether if grew to its present-day size by colliding with a similar size object in the past or by devouring smaller galaxies (e.g. Hughes et al. 2018). Retracing these collision events solely based on the remnants of (dwarf) galaxies could be impossible due to their low surface brightness or moreover, because it is also possible that they might have been dissolved completely (e.g. Boecker et al. 2019). It is, however, thought that during the interaction with the MW, these galaxies deposited some GCs in the MW halo (Abadi et al. 2006). GCs are far more compact than the whole dwarf galaxy, thus are harder to tidally disrupt and, as we have already seen, behave more like point masses in the galaxy and consequently even during galactic collisions. These systems are also easier to spot and then observe and analyse than the dwarf-remnants (Searle & Zinn 1978). For instance, Forbes & Bridges (2010) suggest that 27–47 of the MW GCs were not formed *in situ* but rather originate from 6 to 8 different dwarf galaxies. Similarly, the survey of GCs in other galaxies can be used to understand their evolution process – as, e.g., Prole et al. (2019) did in the case of the Fornax galaxy cluster, or Mackey et al. (2019) in the case of the Andromeda galaxy. The analysis of GCs and the Galactic halo would be also useful in combination with a modelling effort on the waves and warps in the outer Galactic disk (as it is currently studied by the group in Leicester, e.g., Schönrich & Dehnen 2018) because one explanation of this "waviness" is a past interaction of the MW and another (dwarf) galaxy.

GCs undoubtedly possess a wide population of stars of different types and masses from stellar-mass BHs to white dwarfs (WDs) – as could be inferred from the stellar evolution (e.g. Hurley et al. 2000, 2002) and the IMF which is thought to apply in GCs (e.g. Kroupa 2001), see also Sect. 4.2. Low-mass stars are the most abundant in GCs and due to their substantially long evolution (i.e. $\sim$10 Gyr). Their remnants (i.e. WDs) are, therefore, a useful probe of the age of different populations of stars in similarly old objects such as GCs or a host galaxy (e.g. Schmidt 1959; Liebert et al. 1979; Winget et al. 1987). The difficulty in using WDs, however, lies in their low luminosity (on average $M_{\mathrm{V}} \approx 15.5$ mag, Fontaine et al. 2001). Nonetheless, e.g., Kalirai (2012) analysed WDs in the GC M 4 (12.5 Gyr old) and inferred the age of their parent population ($\sim$11.4 Gyr). They further argue that masses and ages of the present-day WDs together with stellar evolutionary models could be used to constrain the time of formation of the (local) MW halo. Using new data from *GAIA*, which is able to identify $\sim 10^5$ WDs in the Solar neighbourhood (Gänsicke et al. 2016), and numerical models of GCs and the MW would lead to more information on the MW formation history.

"What can be said at all can be said clearly, and what we cannot talk about we must pass over in silence."

— Ludwig Wittgenstein

Bibliography

Aarseth, S. J. 1963, MNRAS, 126, 223

Aarseth, S. J. 1972, Binary Evolution in Stellar Systems, ed. M. Lecar (Springer, Netherlands), 88–98

Aarseth, S. J. 2003, Gravitational N-Body Simulations (Cambridge, UK: Cambridge University Press)

Aarseth, S. J. & Zare, K. 1974, Celestial Mechanics, 10, 185

Abadi, M. G., Navarro, J. F., & Steinmetz, M. 2006, MNRAS, 365, 747

Abazajian, K. N., Canac, N., Horiuchi, S., & Kaplinghat, M. 2014, Phys. Rev. D, 90, 023526

Abbate, F., Mastrobuono-Battisti, A., Colpi, M., et al. 2018, MNRAS, 473, 927

Ackermann, M., Ajello, M., Albert, A., et al. 2017, ApJ, 836, 208

Ackermann, M., Ajello, M., Allafort, A., et al. 2012, ApJ, 755, 164

Adams, F. C. & Fatuzzo, M. 1996, ApJ, 464, 256

Ahmad, A. & Cohen, L. 1973, Journal of Computational Physics, 12, 389

Alpar, M. A., Cheng, A. F., Ruderman, M. A., & Shaham, J. 1982, Nature, 300, 728

Amaro-Seoane, P. 2018, Phys. Rev. D, 98, 063018

Anderson, J. & van der Marel, R. P. 2010, ApJ, 710, 1032

Arca-Sedda, M. & Capuzzo-Dolcetta, R. 2018, MNRAS, 2947

Arca-Sedda, M., Kocsis, B., & Brandt, T. D. 2018, MNRAS, 479, 900

Atwood, W. B., Abdo, A. A., Ackermann, M., et al. 2009, ApJ, 697, 1071

Bahramian, A., Heinke, C. O., Sivakoff, G. R., & Gladstone, J. C. 2013, ApJ, 766, 136

Banerjee, S. 2017, MNRAS, 467, 524

Banerjee, S. 2018, MNRAS, 473, 909

Banerjee, S. & Ghosh, P. 2007, ApJ, 670, 1090

Baraffe, I., Chabrier, G., Allard, F., & Hauschildt, P. H. 1998, A&A, 337, 403

Baumgardt, H. 2017, MNRAS, 464, 2174

Baumgardt, H., De Marchi, G., & Kroupa, P. 2008, ApJ, 685, 247

Baumgardt, H., Heggie, D. C., Hut, P., & Makino, J. 2003, MNRAS, 341, 247

Baumgardt, H. & Sollima, S. 2017, MNRAS, 472, 744

Beccari, G., Petr-Gotzens, M. G., Boffin, H. M. J., et al. 2017, A&A, 604, A22

Belczynski, K., Bulik, T., Fryer, C. L., et al. 2010, ApJ, 714, 1217

Belczynski, K., Kalogera, V., Rasio, F. A., et al. 2008, ApJS, 174, 223

Belczynski, K., Repetto, S., Holz, D. E., et al. 2016, ApJ, 819, 108

Belloni, D., Askar, A., Giersz, M., Kroupa, P., & Rocha-Pinto, H. J. 2017, MNRAS, 471, 2812

Binney, J. & Tremaine, S. 1994, Galactic Dynamics (Princeton, New Jersey: Princeton University Press)

Bland-Hawthorn, J. & Gerhard, O. 2016, ARA&A, 54, 529

Boecker, A., Leaman, R., van de Ven, G., et al. 2019, arXiv e-prints, arXiv:1903.11089

Bošković, R. J. 1922, Theoria philosophiae naturalis (A theory of natural philosophy) (Chicago, London: Open Court Publishing Company), latin – English edition from the text of the first Venetian edition, published under the personal superintendence of the author in 1763, with the short life of Boscovich.

Brandt, T. D. & Kocsis, B. 2015, ApJ, 812, 15

Calore, F., Cholis, I., McCabe, C., & Weniger, C. 2015, Phys. Rev. D, 91, 063003

Chandrasekhar, S. 1943, ApJ, 97, 255

Chandrasekhar, S. & von Neumann, J. 1942, ApJ, 95, 489

Chandrasekhar, S. & von Neumann, J. 1943, ApJ, 97, 1

Cohen, R. S., Spitzer, L., & Routly, P. M. 1950, Physical Review, 80, 230

Cohn, H. 1980, ApJ, 242, 765

Cummings, J. D. & Kalirai, J. S. 2018, AJ, 156, 165

Da Rio, N., Robberto, M., Hillenbrand, L. A., Henning, T., & Stassun, K. G. 2012, ApJ, 748, 14

D'Antona, F. & Mazzitelli, I. 1998, Brown Dwarfs and Extrasolar Planets, Astronomical Society of the Pacific Conference Series, 134, 442

Davies, M. B. & Hansen, B. M. S. 1998, MNRAS, 301, 15

De Donder, E. & Vanbeveren, D. 2003, New A, 8, 817

Dehnen, W., Odenkirchen, M., Grebel, E. K., & Rix, H.-W. 2004, AJ, 127, 2753

Desidera, S. & Barbieri, M. 2007, A& A, 462, 345

Dinnbier, F. & Kroupa, P. 2019, in Modelling and Observing Dense Stellar Systems (MODEST-19), conference poster

Duquennoy, A. & Mayor, M. 1991, A&A, 500, 337

Eckner, C., Hou, X., Serpico, P. D., et al. 2018, ApJ, 862, 79

Faber, S. M. & Gallagher, J. S. 1979, ARA&A, 17, 135

Fabian, A. C., Pringle, J. E., & Rees, M. J. 1975, MNRAS, 172, 15

Fabian, A. C., Pringle, J. E., Verbunt, F., & Wade, R. A. 1983, Nature, 301, 222

Flaccomio, E., Damiani, F., Micela, G., et al. 2003a, ApJ, 582, 382

Flaccomio, E., Damiani, F., Micela, G., et al. 2003b, ApJ, 582, 398

Fontaine, G., Brassard, P., & Bergeron, P. 2001, PASP, 113, 409

Forbes, D. A. & Bridges, T. 2010, MNRAS, 404, 1203

Fragione, G. 2019, MNRAS, 483, 3465

Fragione, G., Antonini, F., & Gnedin, O. Y. 2018a, MNRAS, 475, 5313

Fragione, G., Antonini, F., & Gnedin, O. Y. 2019a, ApJ, 871, L8

Fragione, G., Loeb, A., & Ginsburg, I. 2019b, MNRAS, 483, 648

Fragione, G., Pavlík, V., & Banerjee, S. 2018b, ArXiv e-prints, arXiv:1804.04856

Fujii, M. S. & Portegies Zwart, S. 2014, MNRAS, 439, 1003

Gaburov, E., Harfst, S., & Zwart, S. P. 2009, New Astronomy, 14, 630

Gänsicke, B., Tremblay, P., Barstow, M., et al. 2016, in Astronomical Society of the Pacific Conference Series, Vol. 507, Multi-Object Spectroscopy in the Next Decade: Big Questions, Large Surveys, and Wide Fields, ed. I. Skillen, M. Balcells, & S. Trager, 159

Geller, A. M. & Leigh, N. W. C. 2015, ApJ, 808, L25

Gessner, A. & Janka, H.-T. 2018, ArXiv e-prints (arXiv:1802.05274) [arXiv:1802.05274]

Getman, K. V., Flaccomio, E., Broos, P. S., et al. 2005, The Astrophysical Journal Supplement Series, 160, 319

Giersz, M. & Heggie, D. C. 1994, MNRAS, 270, 298

Gnedin, O. Y., Ostriker, J. P., & Tremaine, S. 2014, ApJ, 785, 71

Gong, Y.-X. & Ji, J. 2018, MNRAS, 478, 4565

Goodman, J. & Hut, P. 1993, ApJ, 403, 271

Haghighipour, N. & Raymond, S. N. 2007, ApJ, 666, 436

Hansen, B. M. S. & Phinney, E. S. 1997, MNRAS, 291, 569

Harris, W. E. 1996, AJ, 112, 1487

Heggie, D. C. 1975, MNRAS, 173, 729

Heggie, D. C. 2014 [arXiv:1411.4936v2]

Hénon, M. 1971a, Ap&SS, 13, 284

Hénon, M. 1971b, Ap&SS, 14, 151

Hillenbrand, L. A. 1997, AJ, 113, 1733

Hillenbrand, L. A. & Carpenter, J. M. 2000, ApJ, 540, 236

Hillenbrand, L. A. & Hartmann, L. W. 1998, ApJ, 492, 540

Hills, J. G. 1975, AJ, 80, 809

Hobbs, G., Lorimer, D. R., Lyne, A. G., & Kramer, M. 2005, MNRAS, 360, 974

Hooper, D. & Linden, T. 2016, Journ. Cosm. Astrop. Phys., 8, 18

Hughes, M. E., Pfeffer, J., Martig, M., et al. 2018, Monthly Notices of the Royal Astronomical Society, 482, 2795

Hurley, J. R., Pols, O. R., & Tout, C. A. 2000, MNRAS, 315, 543

Hurley, J. R., Tout, C. A., & Pols, O. R. 2002, MNRAS, 329, 897

Hut, P. 1983, ApJ, 272, L29

Hut, P., McMillan, S., Goodman, J., et al. 1992, PASP, 104, 981

Hénon, M. 1973, A&A, 24, 229

Ito, T., Makino, J., Ebisuzaki, T., & Sugimoto, D. 1990, Computer Physics Communications, 60, 187

Ivanova, N., Heinke, C. O., Rasio, F. A., Belczynski, K., & Fregeau, J. M. 2008, MNRAS, 386, 553

Jalali, B., Baumgardt, H., Kissler-Patig, M., et al. 2012, A&A, 538, A19

Jonker, P. G. & Nelemans, G. 2004, MNRAS, 354, 355

Kalirai, J. S. 2012, Nature, 486, 90

Kaltenegger, L. & Haghighipour, N. 2013, ApJ, 777, 165

Katz, J. I. 1975, Nature, 253, 698

Kirk, H. & Myers, P. C. 2011, ApJ, 727, 64

Kızıltan, B., Baumgardt, H., & Loeb, A. 2017, Nature, 542, 203

Kraus, A. L., Ireland, M. J., Huber, D., Mann, A. W., & Dupuy, T. J. 2016, ApJ, 152, 8

Kroupa, P. 1995, MNRAS, 277, 1507

Kroupa, P. 2001, MNRAS, 322, 231

Kroupa, P., Aarseth, S., & Hurley, J. 2001, MNRAS, 321, 699

Kroupa, P., Jeřábková, T., Dinnbier, F., Beccari, G., & Yan, Z. 2018, A&A, 612, A74

Kroupa, P., Weidner, C., Pflamm-Altenburg, J., et al. 2013, The Stellar and Sub-Stellar Initial Mass Function of Simple and Composite Populations, ed. T. D. Oswalt & G. Gilmore, 115

Küpper, A. H. W., MacLeod, A., & Heggie, D. C. 2008, MNRAS, 387, 1248

Kustaanheimo, P. & Stiefel, E. 1965, Journal für die reine und angewandte Mathematik (Crelles Journal), 1965, 204

Larson, R. B. 1970, MNRAS, 150, 93

Leigh, N. W. C. & Geller, A. M. 2013, MNRAS, 432, 2474

Liebert, J., Dahn, C. C., Gresham, M., & Strittmatter, P. A. 1979, ApJ, 233, 226

Lucy, L. B. 1977, AJ, 82, 1013

Lynden-Bell, D. & Eggleton, P. P. 1980, MNRAS, 191, 483

Lynden-Bell, D. & Wood, R. 1968, MNRAS, 138, 495

Mackey, A. D., Ferguson, A. M. N., Huxor, A. P., et al. 2019, MNRAS, 484, 1756

Makino, J. 1991, PASJ, 43, 859

Makino, J. 1996, ApJ, 471, 796

Makino, J. & Aarseth, S. J. 1992, PASJ, 44, 141

Marzari, F. & Barbieri, D. 2007, A& A, 467, 347

Marzari, F., Baruteau, C., Scholl, H., & Thébault, P. 2012, A& A, 539, A98

Matzner, C. D. & McKee, C. F. 2000, in American Astronomical Society Meeting Abstracts #195, Vol. 195, 135.07

Mayor, M. & Queloz, D. 1995, Nature, 378, 355

McDaniel, A., Jeltema, T., & Profumo, S. 2018, Phys. Rev. D, 97, 103021

McMillan, S., Hut, P., & Makino, J. 1991, ApJ, 372, 111

McMillan, S. L. W. & Lightman, A. P. 1984, ApJ, 283, 801

Mikkola, S. & Aarseth, S. J. 1990, Celestial Mechanics and Dynamical Astronomy, 47, 375

Mikkola, S. & Aarseth, S. J. 1993, Celestial Mechanics and Dynamical Astronomy, 57, 439

Miranda, R. & Lai, D. 2015, MNRAS, 452, 2396

Monaghan, J. J. & Gingold, R. A. 1977, Monthly Notices of the Royal Astronomical Society, 181, 375

Muench, A. A., Lada, E. A., Lada, C. J., & Alves, J. 2002, ApJ, 573, 366

Naoz, S., Farr, W. M., Lithwick, Y., Rasio, F. A., & Teyssandier, J. 2013, MNRAS, 431, 2155

Nelson, A. F. 2000, ApJLett, 537, L65

Nitadori, K. & Aarseth, S. J. 2012, MNRAS, 424, 545

Noyola, E., Gebhardt, K., Kissler-Patig, M., et al. 2010, ApJ, 719, L60

O'Leary, R. M., Stahler, S. W., & Ma, C.-P. 2014, MNRAS, 444, 80

Palla, F. & Stahler, S. W. 1999, ApJ, 525, 772

Papaloizou, J. & Pringle, J. E. 1978, MNRAS, 184, 501

Pavlík, V., Jeřábková, T., Kroupa, P., & Baumgardt, H. 2018, A&A, 617, A69

Pavlík, V., Kroupa, P., & Šubr, L. 2019, arXiv e-prints, arXiv:1905.09289

Pavlík, V. & Šubr, L. 2018, A&A, 620, A70

Peuten, M., Zocchi, A., Gieles, M., Gualandris, A., & Hénault-Brunet, V. 2016, MNRAS, 462, 2333

Pfahl, E. & Muterspaugh, M. 2006, ApJ, 652, 1694

Phinney, E. S. & Kulkarni, S. R. 1994, ARA&A, 32, 591

Picogna, G. & Marzari, F. 2013, A& A, 556, A148

Plummer, H. C. 1911, MNRAS, 71, 460

Plunkett, A. L., Fernández-López, M., Arce, H. G., et al. 2018, ArXiv e-prints

Podsiadlowski, P., Joss, P. C., & Hsu, J. J. L. 1992, ApJ, 391, 246

Podsiadlowski, P., Langer, N., Poelarends, A. J. T., et al. 2004, ApJ, 612, 1044

Portegies Zwart, S. 2011, AMUSE: Astrophysical Multipurpose Software Environment, Astrophysics Source Code Library

Portegies Zwart, S. F. & McMillan, S. L. W. 2000, ApJ, 528, L17

Prisinzano, L., Micela, G., Flaccomio, E., et al. 2008, ApJ, 677, 401

Prole, D. J., Hilker, M., van der Burg, R. F. J., et al. 2019, MNRAS, 484, 4865

Raghavan, D., McAlister, H. A., Henry, T. J., et al. 2010, The Astrophysical Journal Supplement Series, 190, 1

Rasio, F. A., Fregeau, J. M., & Joshi, K. J. 2001, in Astrophysics and Space Science Library, Vol. 264, The Influence of Binaries on Stellar Population Studies, ed. D. Vanbeveren, 387

Repetto, S., Davies, M. B., & Sigurdsson, S. 2012, MNRAS, 425, 2799

Ricker, G. R. et al. 2015, Jour Astron Telescopes, Instruments, and Systems, 1, 014003

Rodriguez, C. L., Zevin, M., Pankow, C., Kalogera, V., & Rasio, F. A. 2016, ApJ, 832, L2

Roell, T., Neuhäuser, R., Seifahrt, A., & Mugrauer, M. 2012, A& A, 542, A92

Salpeter, E. E. 1955, ApJ, 121, 161

Scandariato, G., Robberto, M., Pagano, I., & Hillenbrand, L. A. 2011, A&A, 533, A38

Schmidt, M. 1959, ApJ, 129, 243

Schönrich, R. & Dehnen, W. 2018, MNRAS, 478, 3809

Schuster, A. 1883, Report of the British Association for the Advancement of Science, 53, 427

Searle, L. & Zinn, R. 1978, ApJ, 225, 357

Sigurdsson, S. & Hernquist, L. 1993, Nature, 364, 423

Spitzer, Lyman, J. & Thuan, T. X. 1972, ApJ, 175, 31

Spitzer, Jr., L. 1987, Dynamical evolution of globular clusters

Spitzer, Jr., L. & Hart, M. H. 1971a, ApJ, 164, 399

Spitzer, Jr., L. & Hart, M. H. 1971b, ApJ, 166, 483

Šubr, L., Kroupa, P., & Baumgardt, H. 2008, MNRAS, 385, 1673

Takahashi, K. 1995, PASJ, 47, 561

Tanikawa, A., Heggie, D. C., Hut, P., & Makino, J. 2013, Astronomy and Computing, 3, 35

Tanikawa, A., Hut, P., & Makino, J. 2012, New A, 17, 272

Tauris, T. M. 2011, Evolution of compact binaries. Proceedings of a workshop held at Hotel San Martín, Viña del Mar, Chile 6-11 May 2011. Edited by Linda Schmidtobreick, Matthias R. Schreiber, and Claus Tappert. ASP Conference Proceedings. San Francisco, CA, 447, 285

Tauris, T. M., Langer, N., & Kramer, M. 2012, MNRAS, 425, 1601

Thebault, P. & Haghighipour, N. 2015, Planet Formation in Binaries

Thébault, P., Marzari, F., & Augereau, J.-C. 2010, A& A, 524, A13

Thébault, P., Marzari, F., & Scholl, H. 2008, MNRAS, 388, 1528

Tokovinin, A. 2014a, AJ, 147, 86

Tokovinin, A. 2014b, AJ, 147, 87

Trenti, M., Vesperini, E., & Pasquato, M. 2010, ApJ, 708, 1598

van der Marel, R. P. & Anderson, J. 2010, ApJ, 710, 1063

Varri, A. L., Cai, M. X., Concha-Ramírez, F., et al. 2018, Computational Astrophysics and Cosmology, 5, 2

Verbunt, F., Igoshev, A., & Cator, E. 2017, ArXiv e-prints [arXiv:1708.08281]

Šubr, L., Fragione, G., & Dabringhausen, J. 2019, MNRAS, 484, 2974

Wang, J., Xie, J.-W., Barclay, T., & Fischer, D. A. 2014, ApJ, 783, 4

Winget, D. E., Hansen, C. J., Liebert, J., et al. 1987, ApJ, 315, L77

Xie, J.-W., Payne, M. J., Thébault, P., Zhou, J.-L., & Ge, J. 2011, ApJ, 735, 10

Yuen, D., Wang, L., Chi, X., et al. 2013, GPU Solutions to Multi-scale Problems in Science and Engineering, Lecture Notes in Earth System Sciences (Springer Berlin Heidelberg)

Zapartas, E., de Mink, S. E., Izzard, R. G., et al. 2017, A&A, 601, A29

Ziosi, B. M., Mapelli, M., Branchesi, M., & Tormen, G. 2014, MNRAS, 441, 3703

Zocchi, A., Gieles, M., & Hénault-Brunet, V. 2017, MNRAS, 468, 4429

Zocchi, A., Gieles, M., & Hénault-Brunet, V. 2019, MNRAS, 482, 4713

Attached papers

This attachment contains original papers authored or co-authored by myself that were submitted or accepted for publication to international, peer-reviewed journals and that are relevant to this thesis. The complete list in a chronological order of publication follows:

Pavlík Václav, Jeřábková Tereza, Kroupa Pavel & Baumgardt Holger (2018), *The black hole retention fraction in star clusters*, Astronomy & Astrophysics, Volume 617, A69,
arXiv: 1806.05192, DOI: 10.1051/0004-6361/201832919

Fragione Giacomo, **Pavlík Václav** & Banerjee Sambaran (2018), *Neutron stars and millisecond pulsars in star clusters: implications for the diffuse γ-radiation from the Galactic Centre*, Monthly Notices of the Royal Astronomical Society, Volume 480, 4955–4962,
arXiv: 1804.04856, DOI: 10.1093/mnras/sty2234

Pavlík Václav & Šubr Ladislav (2018), *The hunt for self-similar core collapse*, Astronomy & Astrophysics, Volume 620, A70,
arXiv: 1808.05230, DOI: 10.1051/0004-6361/201833854

Varri Anna Lisa, Cai Maxwell Xu, Concha-Ramírez Francisca, Dinnbier František, Luetzgendorf Nora, **Pavlík Václav**, Rastello Sara, Sollima Antonio, Wang Long & Zocchi Alice (2018), *A MODEST review*, Computational Astrophysics and Cosmology, Volume 5, 2,
arXiv: 1810.07532, DOI: 10.1186/s40668-018-0024-6

Pavlík Václav, Kroupa Pavel & Šubr Ladislav (2019), *Do star clusters form in a completely mass-segregated way?*, Astronomy & Astrophysics, Volume 626, A79
arXiv: 1905.09289, DOI: 10.1051/0004-6361/201834265